AD-A164 170 APPLICATIONS OF WIND EMPIRICAL ORTHOGONAL FUNCTIONS IN TROPICAL CYCLONE MOTION STUDIES(U) NAVAL POSTGRADUATE SCHOOL MONTEREY CA T B SCHOTT DEC 85 1/2

UNCLASSIFIED F/G 4/2 NL

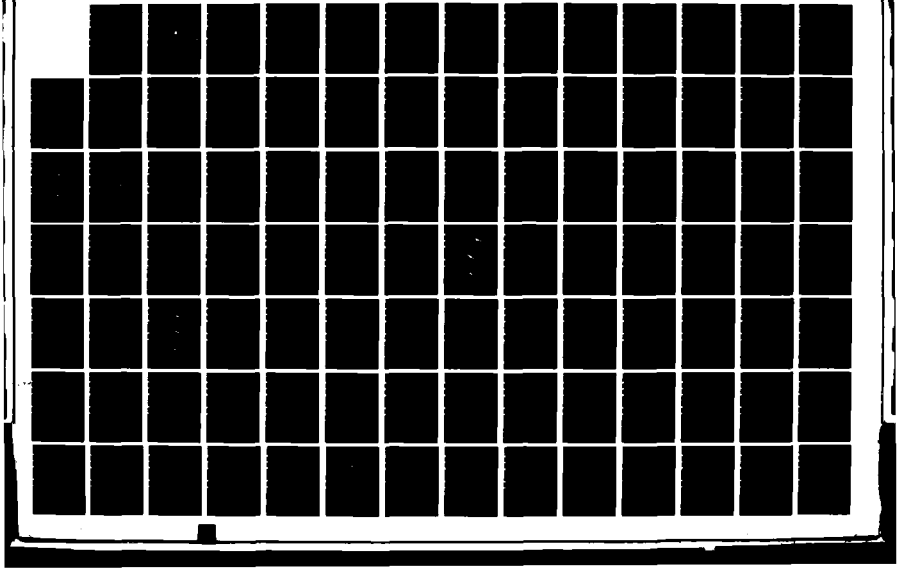

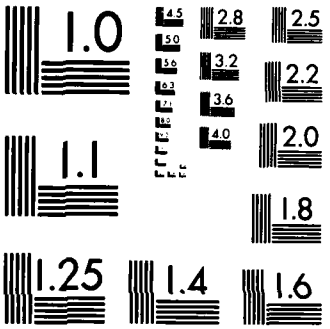

MICROCOPY RESOLUTION TEST CHART

(2)

NAVAL POSTGRADUATE SCHOOL
Monterey, California

THESIS

APPLICATIONS OF WIND EMPIRICAL ORTHOGONAL FUNCTIONS IN TROPICAL CYCLONE MOTION STUDIES

by

Thomas B. Schott

December 1985

Thesis Advisors: R. L. Elsberry
J.C.-L. Chan

Approved for public release; distribution is unlimited

REPORT DOCUMENTATION PAGE

1a. REPORT SECURITY CLASSIFICATION	1b. RESTRICTIVE MARKINGS
2a SECURITY CLASSIFICATION AUTHORITY	3 DISTRIBUTION / AVAILABILITY OF REPORT Approved for public release; distribution unlimited.
2b. DECLASSIFICATION / DOWNGRADING SCHEDULE	
4 PERFORMING ORGANIZATION REPORT NUMBER(S)	5 MONITORING ORGANIZATION REPORT NUMBER(S)
6a. NAME OF PERFORMING ORGANIZATION: Naval Postgraduate School 6b OFFICE SYMBOL (If applicable): 63	7a. NAME OF MONITORING ORGANIZATION: Naval Postgraduate School
6c. ADDRESS (City, State, and ZIP Code): Monterey, California 93943-5100	7b. ADDRESS (City, State, and ZIP Code): Monterey, California 93943-5100
8a NAME OF FUNDING / SPONSORING ORGANIZATION 8b. OFFICE SYMBOL (If applicable)	9. PROCUREMENT INSTRUMENT IDENTIFICATION NUMBER
8c. ADDRESS (City, State, and ZIP Code)	10 SOURCE OF FUNDING NUMBERS PROGRAM ELEMENT NO / PROJECT NO / TASK NO / WORK UNIT ACCESSION NO

11 TITLE (Include Security Classification)

APPLICATIONS OF WIND EMPIRICAL ORTHOGONAL FUNCTIONS IN TROPICAL CYCLONE MOTION STUDIES

12 PERSONAL AUTHOR(S)
Schott, Thomas B.

13a TYPE OF REPORT	13b TIME COVERED	14 DATE OF REPORT (Year, Month, Day)	15 PAGE COUNT
Master's Thesis	FROM _____ TO _____	1985 December	100

16 SUPPLEMENTARY NOTATION

17 COSATI CODES			18. SUBJECT TERMS (Continue on reverse if necessary and identify by block number)
FIELD	GROUP	SUB-GROUP	EOF, tropical cyclone forecasting, regression, post-processing

19 ABSTRACT (Continue on reverse if necessary and identify by block number)

An empirical orthogonal function (EOF) analysis is used to represent environmental wind fields associated with selected western North Pacific tropical cyclones from 1979-1983. Composite synoptic patterns within five past-motion categories of cyclones are studied using 5, 10, 20 and 35 EOF modes. Significant differences in the composite fields are found between categories, which suggests that the wind EOFs are capable of representing synoptic patterns associated with tropical cyclone motion. Regression equations are developed to post-process the forecast track of the One-way Tropical Cyclone Model (OTCM). The predictors for the regression analysis include the EOF coefficients, past motion, storm position, date, intensity, backward extrapolation and forward track displacements. For the dependent sample, the mean 72-h track forecast error for the modified OTCM is 383 km, which represents a 210 km improvement relative to the unmodified OTCM. Thus, the regression scheme has great potential for operational application.

20 DISTRIBUTION / AVAILABILITY OF ABSTRACT	21 ABSTRACT SECURITY CLASSIFICATION
☒ UNCLASSIFIED/UNLIMITED ☐ SAME AS RPT. ☐ DTIC USERS	Unclassified
22a NAME OF RESPONSIBLE INDIVIDUAL: Prof. R. L. Elsberry	22b TELEPHONE (Include Area Code): 408-646-2373 / 22c OFFICE SYMBOL: 63Es

DD FORM 1473, 83 APR edition may be used until exhausted

UNCLASSIFIED

Approved for public release; distribution is unlimited.

Applications of Wind Empirical Orthogonal Functions in Tropical Cyclone Motion Studies

by

Thomas B. Schott
Captain, United States Air Force
B.S., South Dakota State University, 1976

Submitted in partial fulfillment of the
requirements for the degree of

MASTER OF SCIENCE IN METEOROLOGY

from the

NAVAL POSTGRADUATE SCHOOL
December 1985

Author: Thomas B Schott
Thomas B. Schott

Approved by: R L Elsberry
R.L. Elsberry, Thesis Advisor

Johnny C. L. Chan
J.C.-L. Chan, Co-Advisor

R.J. Renard
R.J. Renard, Chairman,
Department of Meteorology

J.N. Dyer
J.N. Dyer,
Dean of Science and Engineering

ABSTRACT

An empirical orthogonal function (EOF) analysis is used to represent environmental wind fields associated with selected western North Pacific tropical cyclones from 1979-1983. Composite synoptic patterns within five past-motion categories of cyclones are studied using 5, 10, 20 and 35 EOF modes. Significant differences in the composite fields are found between categories, which suggests that the wind EOFs are capable of representing synoptic patterns associated with tropical cyclone motion. Regression equations are developed to post-process the forecast track of the One-way Tropical Cyclone Model (OTCM). The predictors for the regression analysis include the EOF coefficients, past motion, storm position, date, intensity, backward extrapolation and forward track displacements. For the dependent sample, the mean 72-h track forecast error for the modified OTCM is 383 km, which represents a 210 km improvement relative to the unmodified OTCM. Thus, the regression scheme has great potential for operational application.

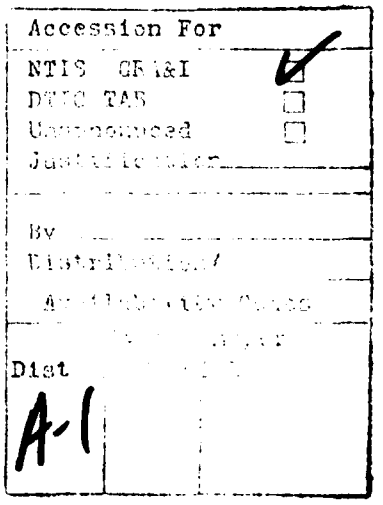

TABLE OF CONTENTS

ACKNOWLEDGEMENTS

I wish to thank Drs. Russ Elsberry and Johnny Chan who directed my research. It was their guidance that made it possible for me to accomplish this research. They taught me that the answers to difficult problems are within my reach and that they can be attained by thorough research and hard work.

I am grateful to Jim Peak for the numerous times he helped me with my computer problems. He was always willing to take time out of his busy schedule to help me. Jim is also responsible for many of the computer subroutines used in my research. In particular, his CT/AT component and revised CLIPER subroutines were easily adapted for my use.

I would also like to thank the people who contributed the data sets used in this research. Dr. Ted Tsui, Naval Environmental Prediction Research Facility, prepared a comprehensive data set which contained the forecasts from various aids used by the JTWC. Lt. William Wilson accomplished the EOF analysis and organized the wind fields used in this study. It was his research that laid the ground work for my study.

Finally, I would like to dedicate this work to my wife, Deb Schott. She managed to give me encouragement when I needed it the most. For two years she did not complain as I dedicated my life to the pursuit of knowledge. Deb, you made it possible. Thank you!

I. INTRODUCTION

A. BACKGROUND

One of the most difficult problems in tropical meteorology is to forecast the movement of tropical cyclones. Although operational tropical cyclone track forecasting remains rather subjective, a number of objective forecast aids provide guidance as to the future storm track. No one forecast aid has yet provided consistent guidance in the wide variety of observed weather situations. Each aid has strengths and weaknesses. Better tropical cyclone forecasts hinge on a better utilization of existing forecast aids (Neumann and Pelissier, 1981; Tsui, 1984).

In this study, synoptic information is used to develop a statistical-synoptic forecast technique which will be used to modify an existing forecast aid used by the Joint Typhoon Warning Center (JTWC) in Guam. The modification scheme (see Chapter 4) should enable the JTWC forecaster to better utilize the existing aid. It is appropriate to give a brief overview of the forecast aids that use synoptic information to make cyclone track forecasts. The original statistical-synoptic techniques (e.g., Riehl et al., 1956) used latitudinal and longitudinal differences of geopotential values to estimate the steering components of the storm. Two examples in use today by the National Hurricane Center (NHC) are the NHC67 and NHC72 models. These models use the current and 24-h old 1000, 700 and 500 mb geopotential height data to modify a preliminary forecast based on climatology and presistence (Neumann and Pelissier, 1981). In these models, the most significant geopotential heights, which are positioned across the storm, act as steering predictors.

Statistical-synoptic techniques typically use a grid that is relocated each forecast period so that the storm is

always at the same gridpoint. Synoptic data, such as geopotential height values, are subjectively or objectively interpolated onto the grid. The gridpoint values are then used to develop regression equations to predict zonal and meridional displacements of the storm. The regression analysis typically chooses only a few key gridpoint values. Therefore, this approach incorporates only a small portion of the original synoptic field.

The synoptic-scale data used in statistical-synoptic models have not been limited only to analyses at the forecast time. The NHC73 model uses numerically predicted values (from a global model) as potential predictors (Neumann and Lawrence, 1975). The NHC73 model has proven to be one of the most consistent methods in the Atlantic region (Neumann and Pelissier, 1981).

Synoptic-scale information is also used in some analogue-type prediction schemes. Analogue techniques are based on the assumption that a tropical cyclone will move similar to previous storms that occurred within some spatial region and temporal interval of the current storm. A computer algorithm searches numerous cases until a family of storms is found with the same general characteristics as the current storm. The storm is then forecast to move along the weighted mean track of the family of storms. An example of an analogue routine that uses synoptic information was described by Jarrell and Somervell (1970). They included the location of the subtropical ridge and midlatitude trough in their routine. A weakness in these analogue techniques is the failure to give a forecast under anomalous conditions.

In all of the statistical techniques discussed above, the synoptic field has been represented by gridpoint values. Only selected points from the field, or a characterization of the field such as the latitude of the trough line, have

been used. Adjacent gridpoints in the field may be highly correlated, and thus not provide independent information.

An alternate approach to a gridpoint representation of a synoptic field has been described by Shaffer (1982). He used empirical orthogonal function (EOF) analysis to represent the 500 mb geopotential height fields on a grid centered on the tropical cyclone. Shaffer and Elsberry (1982) demonstrated that the coefficients from the EOF analysis could be used as synoptic forcing predictors in a statistical-synoptic track prediction scheme.

In a similar study, Wilson (1984) used EOF analysis to represent the 700, 400 and 250 mb wind component fields on a grid centered on the tropical cyclone. Wind fields may have greater utility than geopotential height fields in the tropics because the geopotential height gradients are weak and the flow is far from geostrophic. This is especially true for smaller scale motions such as tropical cyclones. Wilson demonstrated that the coefficients from the wind EOF analysis could be used as synoptic forcing predictors in a statistical track prediction scheme.

The numerical model is another type of track forecast scheme that uses synoptic information. One of the first numerical models was the SANBAR barotropic model, which was based on the assumption that momentum advection is the primary physical mechanism for motion of intense tropical cyclones (Sanders and Burpee, 1968). This simple single-level model steers the storm based on the large-scale, vertically-integrated current in which it is embedded.

Recently, several meteorological agencies have successfully applied fine-resolution or nested numerical models to the problem of predicting tropical cyclone movement. The National Meteorological Center (NMC) uses a Moveable Fine Mesh (MFM) model. The fine mesh grid is

relocated relative to the storm center during a forecast. The MFM has 10 vertical layers and includes physical processes similar to the primitive equation models used in mid-latitudes. The U. S. Navy's Fleet Numerical Oceanography Center (FNOC) has two numerical models for predicting tropical cyclone movement. The One-way Tropical Cyclone Model (OTCM) is discussed in detail in Chapter 4. Although the OTCM is a three-layer, primitive equation model (Hodur and Burk, 1978), it has proven to be one of the best forecast aids used by the JTWC (Tsui, 1984; Peak and Elsberry, 1986). The other dynamical tropical cyclone model used by the Navy is the two-way interactive Nested Tropical Cyclone Model (NTCM). The model uses a fine resolution grid (41 km) near the tropical cyclone and a coarse grid (205 km) away from the cyclone. The initial results of the NTCM were described by Harrison (1981).

Numerical weather prediction in the tropics has not been as successful as mid-latitude numerical prediction for a number of reasons. Tropical regions have very poor data coverage compared to the mid-latitude regions. This results in a poorly defined initial field for the tropical model. Another problem is that the physical processes involved in tropical circulations are not fully understood.

In summary, several forecast schemes use synoptic information to forecast the movement of tropical cyclones. These forecast models range from statistical to numerically based schemes. The major weakness of statistical schemes is forecasting for anomalous conditions, while dynamical forecasting tends to exhibit systematic errors. Since the systematic errors are repetitive, a statistical post-processing scheme (see Chapter 4) may be used to reduce these errors.

B. OBJECTIVES

The current tropical cyclone forecast requirements for JTWC are summarized by Sandgathe (1985). Accurate 48-hour forecasts are normally required for air and naval base evacuation and preparation. Accurate 72-hour forecasts are required for ship routing and major operational exercises. Better accuracy in the forecasts is desirable to avoid costly multiple evacuations of aicraft or overloading of strategic bases. Guided by the current requirements at JTWC, this study will concentrate on improving the accuracy of forecasting the cyclone position at the 72-h interval. One of the primary forecast aids at JTWC is the One-way Tropical Cyclone Model (OTCM). A method that can help the JTWC forecaster better utilize the OTCM would be beneficial. Therefore, a goal of this study is develop a modification scheme for the OTCM. Any improvement in the OTCM forecasts should be beneficial, since it has proven to be one of the best forecast aids used by JTWC (Tsui, 1984; Peak and Elsberry, 1986).

The same data set used by Wilson (1984) is used in this study. It consists of EOF coefficients based on synoptic wind information, along with the appropriate tropical cyclone information. A detailed description of the data set is found in Chapter 2. The first step in this research is to demonstrate that the wind-based EOF coefficients can be used to define synoptic effects acting on tropical cyclones. One advantage of EOF analysis (see Chapter 2) is a considerable reduction in the storage required to represent the synoptic forcing, as the entire wind field surrounding the tropical cyclone can be defined by a small set of EOF coefficients. A compositing technique using the EOFs to define the synoptic forcing of the tropical cyclone track is presented in Chapter 3. The second step in this study is to utilize the synoptic description in terms of the wind EOFs

to adjust the OTCM (see Chapter 4). A successful post-processing scheme should provide the JTWC forecaster with guidance as to when and how the OTCM forecast should be modified. Finally, Chapter 5 addresses the implementation of the OTCM post-processing technique and suggests future research related to this study.

To summarize, there are two objectives for this study. First, demonstrate that the EOF coefficients can be used to differentiate between synoptic situations affecting tropical cyclone motion. The second objective is to derive a statistical post-processing scheme for modifying the OTCM.

II. DATA AND METHODS OF STUDY

A. DATA ACQUISITION AND FIELD DEFINITION

This study employs the same data set used by Wilson (1984). Western North Pacific tropical cyclone information from 1979-1983 is obtained from the annual tropical cyclone reports published by the Joint Typhoon Warning Center (JTWC) in Guam. The data set includes warning and best-track positions at six-hour intervals, as well as the estimated intensity of the storm (maximum sustained winds).

The U. S. Navy's Fleet Numerical Oceanography Center provided operational wind fields from the Global Band Analyses (GBA). The GBA wind fields are produced every 12 h on a Mercator projection true at 22.5°N. The grid resolution is 2.5° longitude by approximately 2.5° latitude. The GBA provide complete longitudinal coverage between 41°S and 59.8°N. When a tropical cyclone is present, eight bogus winds at the surface are inserted at 80 km from the center of the cyclone, and vertical coupling is achieved via the thermal wind relation using temperature analyses at intermediate levels. Upper-air observations include rawinsondes, pibals, aircraft and cloud motion vectors. In regions with no observations, the analysis will be a blend of the 12 h old analysis and 5% climatology. The interested reader can refer to the U.S. Naval Weather Service (1975) for a detailed description of the GBA. The GBA fields are available for the zonal and meridional wind components at 00 and 12 GMT since 1975. For this study, only data between 1979-1983 at 700, 400 and 250 mb are used.

Several criteria are imposed in selecting a storm for inclusion in the data set. A tropical cyclone must have matured to at least tropical storm intensity (maximum sustained winds of 18 m/s or greater) and must have been

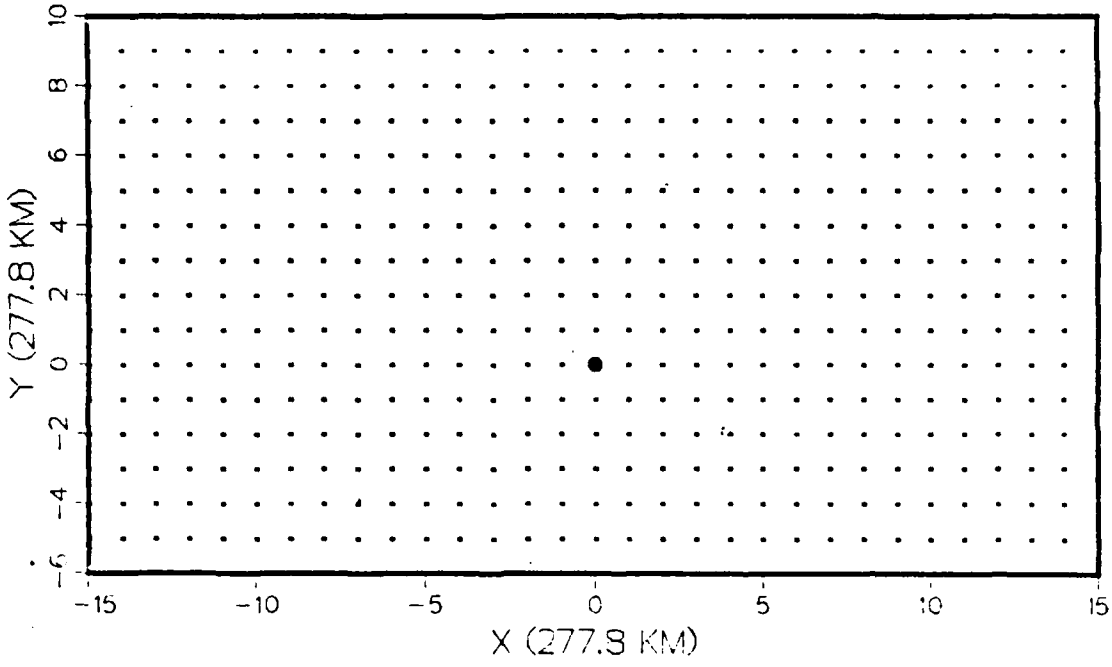

Fig. 2.1. The relocatable 527-point grid with a fixed zonal and meridional separation of 277.8 km. The vortex center (0,0) is located at gridpoint (16,9) from the lower left corner, and is indicated by the large dot.

west of the dateline. The GBA must have been available for the zonal and meridional wind components at 700, 400 and 250 mb. Finally, the JTWC warning position at 00 or 12 GMT must have been at a latitude south of 34.6°N. This latter restriction is necessary to ensure that the GBA winds are available for a sufficient latitudinal extent north of the cyclone center. A total of 1357 cases meet these criteria.

The grid in this study is the same as Wilson's (1984) relocatable grid (Fig. 2.1). It consists of 527 data points with a fixed zonal and meridional separation of 277.8 km (150 n.mi.). There are 31 zonal and 17 meridional gridpoints. For each case, the grid is positioned so that

the tropical cyclone center is always located at the grid point (16,9). The warning position from JTWC is used to indicate the center of the tropical cyclone. For each case that meets the above criteria, the zonal and meridional wind components at 700, 400 and 250 mb are interpolated onto this equidistant grid from the GBA using a bilinear interpolation method (Wilson, 1984).

Recently, statistical studies on tropical cyclone motion have shown an improvement in 24-h forecast errors using a grid system oriented with respect to the initial storm heading (Shapiro and Neumann, 1984). However, the advantages for such a grid system are substantially diminished at the 48 to 72-h forecast times. For this reason, this study uses a geographically-oriented grid. However, five past-motion categories will be used to group similar storm tracks based on the prior 12-h motion.

B. THE EOF METHOD

The method of principal component or empirical orthogonal function (EOF) analysis was first applied to atmospheric sciences by Lorenz (1956). In the past, the EOF analysis has been used as a map typing tool or as a technique for reducing the dimensionality and explaining the variance structure of a field (Wilson, 1984). For example, Stidd (1967) used EOF analysis to describe the variation in average monthly rainfall in Nevada. Brown (1981) divided a large sample into smaller discrete subsets by map typing based on the coefficients derived from the EOF analysis. Other examples include studies by Kutzbach (1967), Hardy and Walton (1978), Legler (1983) and many others.

A one-dimensional data field can be generally represented by simple orthogonal functions such as sines and cosines. Similarly, the eigenvectors derived from EOF analysis can be used to reconstruct a two-dimensional data field. A major advantage in the EOF analysis is that the

eigenvectors are ranked in decreasing order according to the percent of the variance accounted for (Morrison, 1967). For example, the first eigenvector explains the largest variance in the field. The variance unexplained by the first eigenvector would be the residual. The second eigenvector would then explain the maximum variation remaining in the residual field and so on. Since the first few eigenvectors describe a large portion of the total variance in a sample, one may approximate the total field by retaining only these few eigenvectors. As a result, the dimensionality of the data set can be reduced considerably, which makes the EOF method a cost-effective means of representing large data sets.

The procedures for the EOF analysis used in this study follow the treatment outlined by Wilson (1984). A scalar EOF analysis is performed using the zonal (u) and meridional (v) components at 700, 400 250 mb and a sample size of 682 cases. From the 1357 cases that meet the desired criteria, alternate cases within a storm are chosen to make up the 682 cases. At each pressure level and for each wind component, a 527 X 682 matrix A is formed such that the interpolated wind field for a case would appear as a column. The A matrix is normalized by subtracting the sample mean at each gridpoint, and then dividing by the sample standard deviation at that grid point. The normalized matrix Z is then defined with elements z(i,j) given by

$$z(i,j) = (a(i,j)-b(i))/s(i), \qquad (2.1)$$

where a(i,j) are the elements in matrix A and b(i) and s(i) are the mean and standard deviation of the elements in row i of matrix A. In other words, b(i) and s(i) are the mean and standard deviation of the wind component for all the cases at a particular gridpoint i. The normalization of the wind

components in this way ensures that the extratropical regions of the grid, where the variability is generally large, will not dominate the less variable tropical regions in the EOF analysis. A disadvantage in using a standardized matrix is that a small amount of smoothing may occur in the resultant eigenvectors (Kutzbach, 1967).

The symmetric correlation matrix (R) can then be defined by

$$R = ZZ'/n, \tag{2.2}$$

where Z' is the transpose of Z and n is the number of cases. A scalar y can be defined by:

$$y = e'Re, \tag{2.3}$$

where y is the correlation between an arbitrary vector e and the normalized data matrix Z. The vector e has the constraint that it must be normalized to length one (i.e., e'e = 1). It was shown by Morrison (1967) that (2.3) can be written in matrix form as

$$EY = RE. \tag{2.4}$$

In this study, E is a 527 X 527 matrix, and the elements of Y are eigenvalues found by solving $|R - YI| = 0$ (where I is the identity matrix). Each column in E is an eigenvector e associated with a single eigenvalue y_i. In fact, the first eigenvector explains

$$y_1 \Big/ \sum_{i=1}^{m} y_i$$

of the total variance. The second eigenvector explains the largest amount of variance unexplained by the first and so on.

The normalized data matrix Z may be reconstructed by calculating the EOF coefficients or multipliers (Stidd, 1967; and others). These coefficients are found by solving

$$C = E'Z, \tag{2.5}$$

where C is a m by n matrix (527 X 682 for this study). The first column of C is the orthogonal coefficient vector corresponding to the first case, and so on. The normalized matrix Z can now be retrieved by

$$Z = EC. \tag{2.6}$$

The jth case, stored in the jth column of the Z matrix, can be represented by

$$z(i,j) = \sum_{k=1}^{m} e(i,k)c(k,j), \quad i=1,2, \ldots, 527 \tag{2.7}$$

where z(i,j) are the normalized gridpoints values for the jth case, e(i,k) are the elements of eigenvector k, c(k,j) are the coefficients for the jth case and m is the number of modes (eigenvectors) retained.

Since the eigenvectors in E are ranked according to the amount of variance they represent, a large portion of a particular field signal can be represented by a few eigenvectors. Wilson (1984) used the Monte Carlo approach (Preisendorfer and Barnett, 1977) to determine the number of eigenvectors needed to represent the signal of a field and eliminate unnecessary noise. The number of EOF modes that represents signal varies from 19 to 35 depending on the pressure level and wind component field (his Table VI). Wilson demonstrated that retaining only 35 of the 527 EOF modes (eigenvectors) explained between 81.7 to 93.2 percent of the u or v signal at the various pressure levels (his

Table VI). Therefore, only the first 35 EOF modes are used in this study.

Wilson pointed out that the eigenvectors computed with the dependent sample of 682 cases could be used with independent data. However, when a new case is added, the eigenvectors no longer exactly represent the maximum variation of the new plus the old observations. Wilson demonstrated that this does not introduce a significant error as long as the original correlation matrix R is large. The procedure for adding independent data is very similar to that outlined above. The A matrix is formed using the new cases. Each element in A is normalized by the gridpoint mean and standard deviation found from the original cases. The EOF coefficients are then calculated using (2.5), where the E matrix contains the eigenvectors found from the original cases. This procedure is used to determine the EOF coefficients for the remaining 675 cases not used in the original EOF analysis.

C. CT/AT COMPONENTS

Numerous studies have been performed to determine the accuracy of tropical cyclone track forecasts (e.g., Jarrell et al., 1978; Neumann and Pelissier, 1981; Tsui, 1984; and Elsberry and Peak, 1986). Tsui studied the accuracy of various forecast aids used by the JTWC. He considered timing, track, speed and forecast errors. The forecast error was defined as the great circle distance between the forecast and the verifying position. The latter is based on the subjectively smoothed best track, which is produced in a post-storm analysis. Track error is defined as the right-angle distance from the forecast position to the best track. The other error definitions can be found in Tsui (1984). Neumann and Pelissier (1981) introduced another error measurement which involved cross-track (CT) and along-track (AT) components. Elsberry and Peak (1986) used

a similar method to calculate CT/AT components relative to an extrapolated track based on the present and past 12-h warning positions.

In this study, CT and AT components are calculated with respect to a CLImatology and PERsistence (CLIPER) forecast track (Fig. 2.2). A western North Pacific version (called WPCLPR), provided by C. Neumann of the National Hurricane Center, is used (Xu and Neumann, 1985). The CLIPER track forecast is considered as a no-skill forecast, since the scheme does not use any synoptic information (Neumann and Pelissier, 1981). For each case, the CLIPER forecast is made using the -12 and -24 h warning positions, intensity and date of the storm. Warning positions are used because the best-track positions are not available in an operational environment. The CT/AT components are then calculated each 24 h using the best-track positions relative to the CLIPER forecast track. By normalizing the forecast track with CLIPER, the contribution due to climatology and persistence is removed from the forecast.

There are advantages in using a CT/AT component method to measure track forecast errors. The CT component can be thought of as turning motion relative to a CLIPER forecast. A positive (negative) CT component is defined as a best-track position to the right (left) of the CLIPER position at the same forecast time. Thus, the CT component provides a directionality aspect that is not available in the forecast error. Similarly, the AT component can be thought of as an acceleration/deceleration with respect to CLIPER, although a change in direction will produce a negative AT component even when the translation speed remains constant (Neumann and Pelissier, 1981). It is important to note that the CT/AT components are calculated relative to a CLIPER reference at a particular forecast time. That is, the CLIPER reference is different at 24, 48

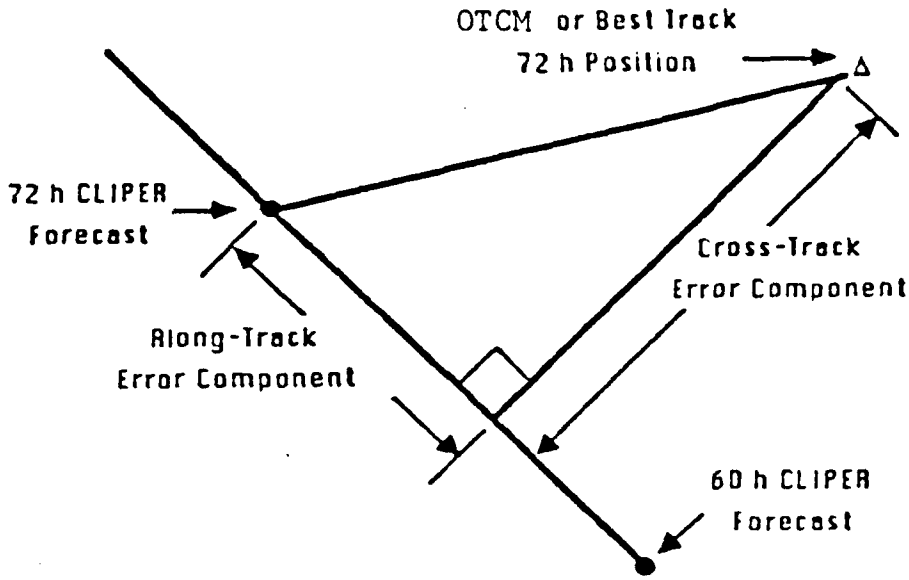

Fig. 2.2. Definition of cross-track and along-track components at 72 h relative to the forecast track based on CLIPER positions at 60 and 72 h. In this example, CT is positive (right) and AT is negative (slow) with respect to the CLIPER track.

and 72 h. The importance of this point will become evident later.

D. PAST-MOTION CATEGORIES

Elsberry and Peak (1986) found from discriminant analysis that the direction and speed of the past 12-h movement were significant predictors of future storm motion. They divided their data set into five "past-motion" categories based on past 12-h track direction and speed (Fig. 2.3). These five categories are used in this study. The basic assumption of the 5-category specification is that the differences in the prior 12-h motion reflect different synoptic forcings. For example, there should be a different environmental forcing between slow- and fast-moving storms.

Likewise, storms moving toward the northeast during the past 12 h should experience a synoptic forcing different from that of a storm moving toward the southwest or south.

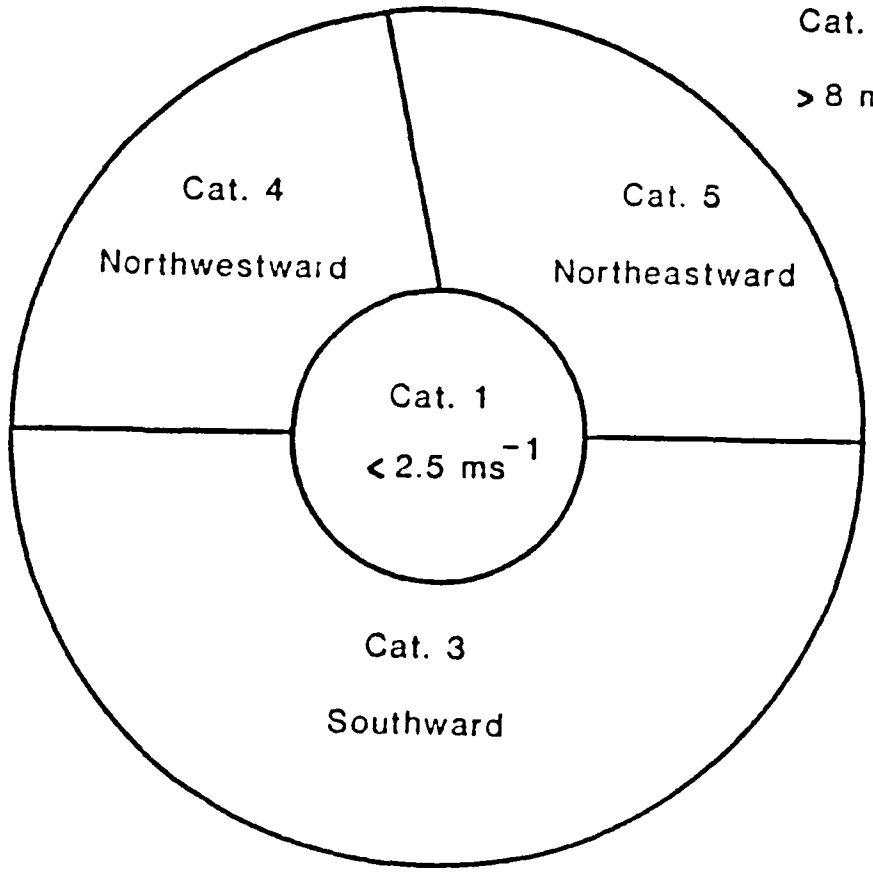

Fig. 2.3. Schematic of the five past-motion categories based on the past 12-h speed (Categories 1 and 2) and direction (Categories 3-5) of the tropical cyclone.

The entire sample of 1357 cases is sorted according to the past 12-h motion categories defined in Fig. 2.3. Categories 1 (slow) and 2 (fast) are the speed categories, where speed is defined as the translation speed from -12 h

to 00 h warning positions. The storms with weak and strong steering currents should be isolated in these two categories. Categories 3, 4 and 5 are the directional categories. For example, storms translating northwestward between 2.5 and 8 m/s will be in Category 4. A summary of sample sizes in each of the past-motion categories is found in Table 1. The largest sample size is found in Category 4. The remaining categories have considerably fewer cases. Notice that 155 cases are not classified into any of five past-motion categories because these cases in the original Wilson (1984) were missing a past 12-h warning position.

Table 1. Sample sizes of the five past-motion categories defined by the past 12 h motion of the cyclone.

Category	Sample Size
1 (<2.5 m/s)	169
2 (>8.0 m/s)	174
3 (80-270°)	125
4 (270-340°)	497
5 (340-80°)	237
Total	1202

The mean characteristics of the storms within these past-motion categories are summarized in Table 2. The mean and standard deviation for the speeds of the storms in Categories 3, 4 and 5 are approximately the same. Because of the large variance in track direction for the Slow and Fast categories, their mean directions are not calculated. The mean intensities of cyclones in Categories 1, 4 and 5 appear to be higher. However, the standard deviations in these categories are also larger. Therefore, it is unlikely that the mean intensities between categories are

significantly different. There is also a slight tendency for storms in Categories 2 and 5 to be initially farther north and west than the other categories, but again the standard deviations are large.

Table 2. Mean ($\bar{X}$) and standard deviations (σ) within each of the five past-motion categories.

Parameter	Cat	$\bar{X}$	σ
Speed (total) (m/s)	1	1.6	0.6
	2	10.9	3.5
	3	4.9	1.6
	4	5.0	1.4
	5	4.7	1.4
Speed (x-dir) (m/s)	1	-0.5	1.1
	2	-3.2	9.4
	3	-3.4	3.4
	4	-4.1	1.5
	5	1.4	2.0
Speed (y-dir) (m/s)	1	0.5	1.1
	2	4.4	3.6
	3	-1.3	1.5
	4	2.4	1.4
	5	4.0	1.5
Direction (degrees)	3	233	53
	4	301	18
	5	20	27
Intensity (kt)	1	62	26
	2	58	24
	3	56	27
	4	69	31
	5	64	26
Initial Longitude (°E)	1	131	14
	2	136	12
	3	131	15
	4	132	13
	5	136	14
Initial Latitude (°N)	1	17	6
	2	20	8
	3	16	5
	4	17	5
	5	20	7

The firtst 50 storm tracks within each of the five categories are illustrated in Figs. 2.4 and 2.5. Composite

wind fields for each of the categories will be presented later. Most of the storms in the fast category (Category 2) initially moved either toward the northeast or the northwest. Therefore, the synoptic flow patterns in this fast category might be smoothed when adding wind fields associated with the northeast- and northwest- moving storms. Notice the general rotation of the past 12-h tracks for the storms in Categories 3, 4 and 5 (Fig. 2.5). However, there are a variety of future tracks within each category.

Many of these forecast situations will not have a verifiable 72-h position. Within this sample, only about 25% of the storms have a +72-h position (Table 3). More than 30% of the storms in the fast (Category 2) and northeast (Category 5) categories do not even have a +24-h position. These differences in storm lifetimes need to be considered when interpreting the composites in the following section.

Statistical properties of the CT/AT components within each past-motion category are summarized in Table 4. The largest sample size is in Category 4 (northwestward) and the smallest is in Category 3 (southward). In general, the overall means and standard deviations of CT components for each time period are smaller than those found by Elsberry and Peak (1986), who calculated the CT/AT components relative to an extrapolation track. As shown in Table 4, the mean CT components are near zero and do not increase markedly with time when the CLIPER track is used as a reference. The CLIPER normalization also reduces the means and standard deviations for the AT components within each category and time period compared to those in the Elsberry and Peak (1986) study. Therefore, normalization with respect to the CLIPER track maybe superior to the use of a extrapolation track. Notice that the largest standard deviations occur in Category 2 (fast), which is consistent

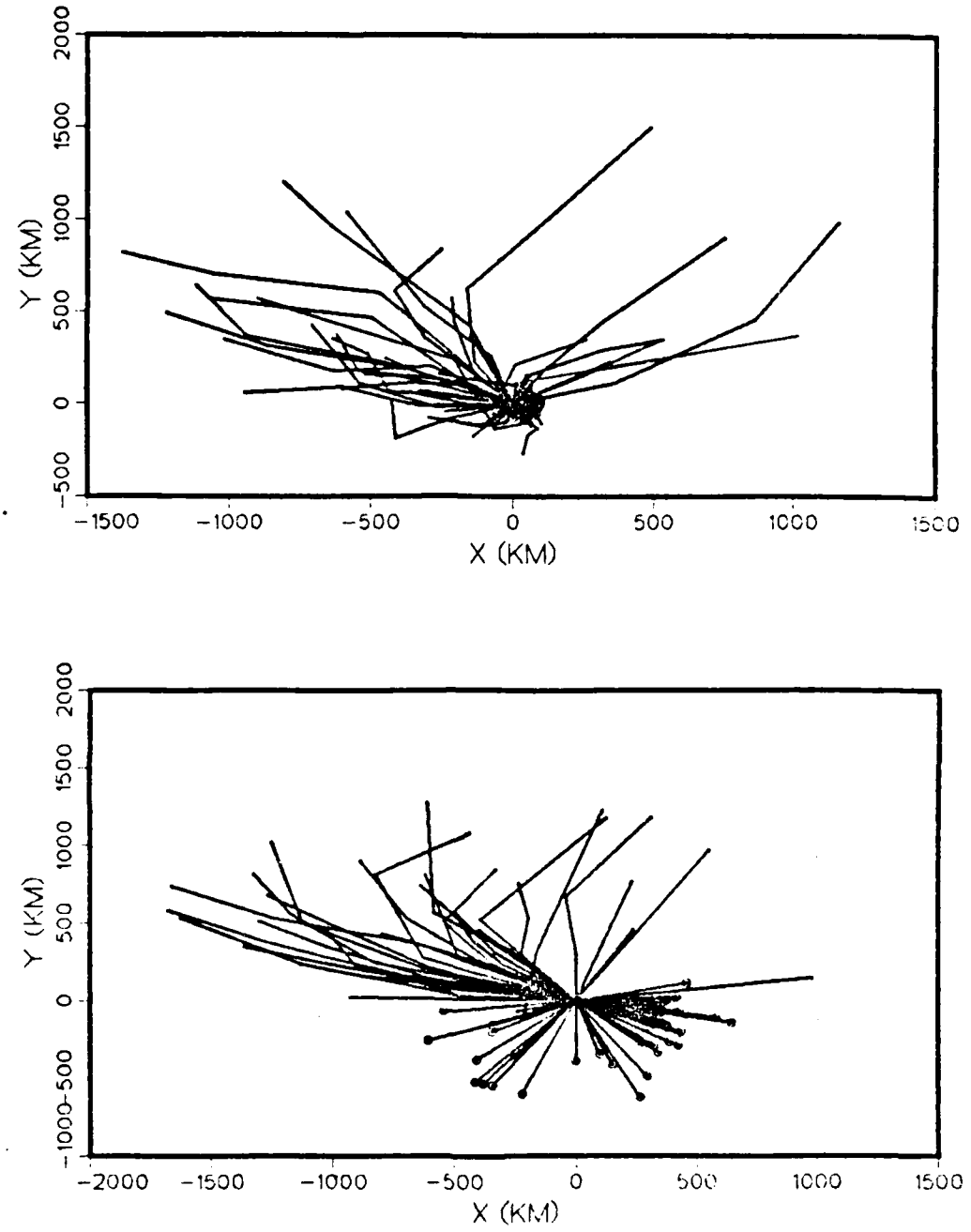

Fig. 2.4. 50 storm tracks from Category 1 (top) and Category 2 (bottom). Points plotted are -12 and 00 warning positions, and 24, 48 and 72 best-track positions, as available. The large dots indicate the -12 h positions.

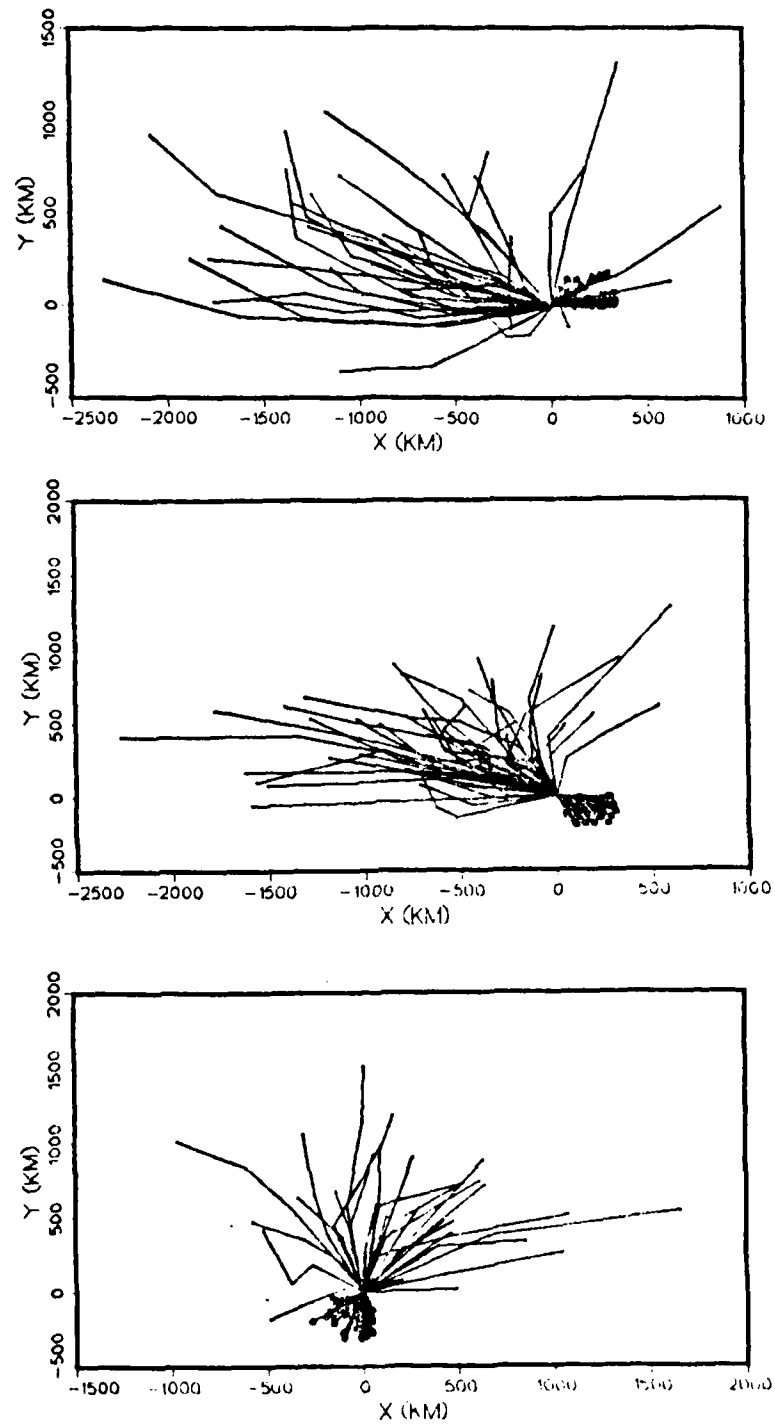

Fig. 2.5 As in Fig. 2.4, except for Category 3 (top), Category 4 (middle) and Category 5 (bottom) storms.

Table 3. Number of the 50 storms within each category in Figs. 2.4 and 2.5 that have verified positions at 24, 48 and 72 h.

	Time (h)		
Category	24	48	72
1 (<2.5 m/s)	42	33	30
2 (>8.0 m/s)	32	23	16
3 (80-270°)	39	35	29
4 (270-340°)	45	39	34
5 (340-80°)	34	22	12

with the wide variety of track positions at 72 h (Fig. 2.4). Some of these storms continued to move rapidly, while others slowed down and began to recurve.

Histograms of CT and AT provide a graphic representation of the data presented in Table 4. For example, the Category 4 frequency distributions are shown in Fig. 2.6. It will be shown later that it is useful to subdivide the CT/AT components into three equal subcategories (terciles) within a category. The CT component terciles are to the left, center and right of the CLIPER track. For example, one third of the Category 4 CT72 sample is located in the central tercile category bounded by CT72 values of -155 and 108 n mi. The storm characteristics within each of these tercile subcategories will be studied later. A similar division into slow, center and fast terciles relative to CLIPER is made for the AT72 components. Since the tercile sample sizes become very small in all categories except Category 4, conclusions regarding the other tercile categories should be viewed as tentative until larger samples can be tested. Therefore, only tercile subcategories within Category 4 will be examined in this study.

Table 4. Statistical properties of 24, 48 and 72 h CT and AT components (n mi) for the past- motion categories defined in Fig. 2.3. The central one third of the tercile sample lies between the cutpoints. (N, sample size; $\bar{x}$, mean; σ, standard deviation). Overall summary is for all five past-motion categories of storms during 1979-1983.

			CT		AT		Tercile Cutpoints CT		AT	
Time	Cat	N	$\bar{X}$	σ	$\bar{X}$	σ	Left	Right	Slow	Fast
24	1	135	-19	86	-20	89	-56	14	-50	14
	2	84	5	119	-80	171	-26	46	-116	-4
	3	74	7	88	14	112	-31	40	-30	59
	4	367	-4	90	-22	80	-41	35	-54	6
	5	150	1	102	-46	117	-20	44	-81	-3
overall		810	-2	97	-31	114				
48	1	112	-21	159	-91	204	-75	48	-154	13
	2	66	-22	251	-22	292	-85	101	-120	36
	3	64	1	224	45	208	-90	92	-45	118
	4	304	-12	181	-60	171	-88	57	-120	0
	5	90	17	201	-140	201	-29	115	-201	-60
overall		636	-7	203	-54	215				
72	1	95	-17	249	-198	319	-90	70	-283	-34
	2	54	-20	380	-287	585	-166	184	-293	-82
	3	57	-41	361	3	236	-169	140	-102	109
	4	235	-15	300	-114	250	-155	108	-184	-7
	5	58	-14	292	-160	265	-109	87	-281	-115
overall		499	-21	316	-151	331				

The mean characteristics of the storms in the CT72 and AT72 tercile subcategories of Category 4 are shown in Table 5. No significant differences in the past-motion characteristics can be identified to explain the tercile subcategories. That is, the mean differences are small and the standard deviations are large compared to the mean. Thus, the storm characteristics at the observation time and -12 h do not give a clear indication of the deviations of the 72 h position with respect to a CLIPER track. It will be demonstrated below that the composite synoptic wind fields do provide a discriminator of future motion.

When using an extrapolated track based on past 12-h motion, Elsberry and Peak (1986) found that a majority of

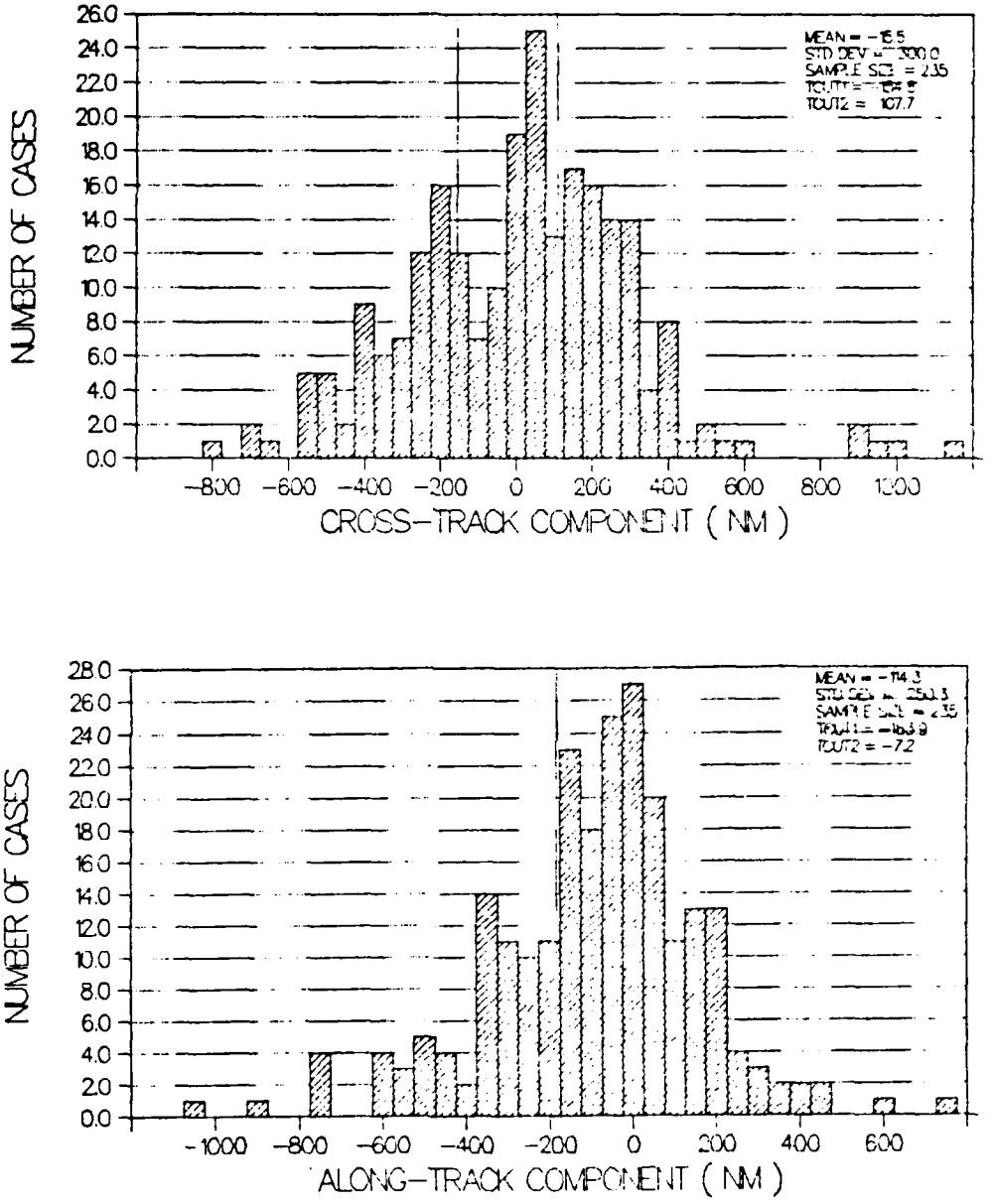

Fig. 2.6. Histogram of the 72-h cross-track (top) and along-track (bottom) components (n.mi.) for Category 4 storms during 1979-1983. Vertical lines indicate the tercile cutpoints (TCUT1 and TCUT2) for the sample.

Table 5. Means ($\bar{X}$) and standard deviations (σ) of the past 12-h characteristics of Category 4 storms within each of the CT or AT terciles at 72 h.

Parameter	Cat	$\bar{X}^{CT72}$	σ	Cat	$\bar{X}^{AT72}$	σ
Speed (total) (m/s)	Left	5.2	1.4	Slow	4.7	1.4
	Center	4.8	1.4	Center	5.0	1.3
	Right	4.8	1.3	Fast	5.0	1.4
Speed (x-dir) (m/s)	Left	-4.3	1.6	Slow	-3.9	1.5
	Center	-4.0	1.5	Center	-4.2	1.4
	Right	-4.0	1.4	Fast	-4.2	1.6
Speed (y-dir) (m/s)	Left	2.3	1.5	Slow	2.2	1.4
	Center	2.3	1.3	Center	2.4	1.4
	Right	2.4	1.3	Fast	2.3	1.3
Direction (degrees)	Left	299	19	Slow	301	18
	Center	300	17	Center	299	17
	Right	301	16	Fast	300	18
Intensity (kt)	Left	73	31	Slow	77	33
	Center	81	31	Center	77	31
	Right	73	33	Fast	73	32
Initial Longitude (°E)	Left	136	11	Slow	139	14
	Center	134	11	Center	133	9
	Right	135	10	Fast	134	7
Initial Latitude (°N)	Left	14	4	Slow	14	4
	Center	16	4	Center	16	4
	Right	15	3	Fast	15	5

Table 6. Distribution of 235 Category 4 cyclones within cross-track and along-track (AT72) terciles.

		AT72		
		Slow	Center	Fast
	Left	25	22	30
CT72	Center	28	31	20
	Right	24	26	29

the cases in the AT72 fast tercile category were also in the CT72 right category. Such a correlation would be expected for recurving storms in the extrapolation coordinate system. The AT and CT distributions of cases at 72 h, using a CLIPER coordinate system, are given in Table 6. The fast AT72 cases are fairly well distributed in all three CT72 and AT72 terciles. In fact, a bias within the CT72 and AT72 terciles cannot be demonstrated. This indicates that the tercile subcategories, formed using a CLIPER coordinate system, provides a better normalization of the 72-h storm positions than does the extrapolation coordinate system used by Elsberry and Peak (1986).

III. DATA ANALYSIS

An objective of this study is to demonstrate the usefulness of the wind-based EOFs for defining the synoptic flow associated with tropical cyclone motion. Shaffer and Elsberry (1982) suggested that the environmental flow around the tropical cyclone could be described by a small set of EOF coefficients based on geopotential height fields. They demonstrated that certain eigenvectors were correlated with zonal motion of the tropical cyclone, whereas others were related to meridional motion. For example, if the EOF coefficient 1 is large and positive, the storm initially moves northwestward (their Fig. 6). On the other hand, a storm tends to move towards the northeast when the EOF coefficient 1 is small or negative. Peak and Elsberry (1986) applied a regression analysis to predict the future motion of the cyclone in cross-track and along-track tercile categories using EOF coefficients derived from geopotential fields as predictors. A second regression scheme was developed to predict CT and AT components within past-motion categories defined in Fig. 2.3. These sets of regression equations provided better track forecasts than those from the first set which did not use the past-motion categorization. Based on these studies, it seems reasonable to examine the synoptic effects in terms of wind-based EOF coefficients for cases within categories defined by the past 12-h motion of the storm.

To demonstrate that the eigenvectors represent a synoptic effect on cyclone motion, composite wind fields are calculated using the EOF coefficients. Although compositing smooths features particular to individual cyclones, the features common to all the cyclones in a synoptic category should be evident. By comparing composite fields for each

of the five synoptic categories, it should be possible to demonstrate that a small set of the EOF eigenvectors can be used to represent differences in synoptic forcing between categories.

The cases in the data set are identified by the date-time group and category of past storm motion, so that the selection of all the cases in a particular storm motion category is easily accomplished. Each case in the sample also has a set of (the first) 35 u and v EOF coefficients for each of the three pressure levels (i.e., 700, 400 and 250 mb). For example, the 700 mb EOF coefficients 1 through 35 may be used to reconstruct the u-component wind field (Wilson, 1984) for a given case.

Since the wind-based EOF coefficients (modes) are linear, two composite methods are possible. Summation of the magnitude of individual EOF coefficients for the cases in a category, then divided by the number of cases, would yield the mean EOF coefficients. The composite field could then be reconstructed by multiplying these mean coefficients by the eigenvectors. The alternative method would be to reconstruct the fields for each of the cases in a category, sum and divide by the number of cases. Both methods will yield the same result. The latter method is chosen because it is the traditional method of compositing for meteorological fields. This method will be discussed in more detail.

The composite technique follows the EOF reconstruction procedures outlined in Chapter 2. In particular, the wind component field is reconstructed gridpoint by gridpoint. The normalized wind component for a particular case (j) at the gridpoints z(i,j) can be reconstructed from the EOF eigenvectors by

$$z(i,j) = \sum_{k=1}^{m} e(i,k)\, c(k,j) \qquad i=1,2, \ldots, 527 \qquad (3.1)$$

where c(k,j) are the EOF coefficients for the jth wind component field and e(i,k) are the appropriate eigenvectors. Conversion to a dimensional wind component is accomplished by

$$a(i,j) = z(i,j)s(i) + b(i) \quad i=1,2, \ldots, 527, \qquad (3.2)$$

where b(i) and s(i) are the mean and standard deviation of the elements in row i of matrix A. As will be shown later, it is possible to make composite fields using any number of coefficients (e.g. 5, 10, 20, 35, ..., 527). All of the variance in the original field would be described by including all 527 coefficients. The procedure outlined above is repeated for each case in the data set. Composite fields are then formed by adding each field and dividing by the number of cases in the composite.

A. PAST-MOTION CATEGORY COMPOSITES

The composite 700 mb u and v fields for Categories 4 and 5 are shown in Figs. 3.1 and 3.2. The mean u field (Fig. 3.1) for the northwest-moving (Category 4) storms has a strong easterly component throughout the center of the grid, whereas the northeast movers (Category 5) have weaker easterly components. The most striking feature in the v field (Fig. 3.2) is that the southerly component east of the vortex is stronger in the Category 5 composite even though the mean intensities of the storms are approximately the same in these categories (see Table 2). Tropical cyclones moving with a northward bias (Category 5) should have a stronger southerly component and a weaker easterly component than those moving with a westward bias (Category 4). Therefore, the observations in the mean u and v composites are physically consistent with the mean directions of Category 4 (301°) and Category 5 (20°). Thus, the 35 wind-based EOFs represent differing synoptic environments of the tropical cyclone.

The composite vector wind fields (Fig. 3.3) also provide insight into the synoptic differences between the past-motion categories. The subtropical ridge is east of the vortex in Category 5, but farther to the northeast for Category 4. Both composites show a convergence area to the southeast of the vortex. The composites tend to smooth any midlatitude trough and ridge patterns in the northern part of the grid, along with other circulation features that are not found consistently in the same location relative to the tropical cyclone. However, the mean wind field for Category 5 gives a stronger indication of a trough to the north of the vortex. The cyclonic circulation around the vortex also extends over a larger area in the Category 5 composite. Thus, the radial extent of the average vortex in Category 5 may be greater than that found in Category 4. A similar result appears in Chan (1985), who found that the cyclones in his northward motion stratification were on the average larger than those with a westward motion.

Subtraction of the composite wind fields from the two categories indicates regions with differences in synoptic forcing (Fig. 3.4). For example, the largest differences (5 to 5.5 m/s) are found to the northeast of the vortex. If the wind distribution at each gridpoint is assumed to be normal, it is possible to determine statistically if the u or v component is significantly different at a gridpoint using a Student's t-test. The null hypothesis is that there is no significant difference in the mean wind components between the two categories. If the mean and standard deviation at a particular gridpoint yields a t-value of greater than 1.96 (95% confidence limit for the sample sizes in Table 1), the wind component at that gridpoint would be statistically different between the two samples. At least one of the two components is significantly different between Categories 4 and 5 at 433 of the 527 gridpoints in Fig. 3.4.

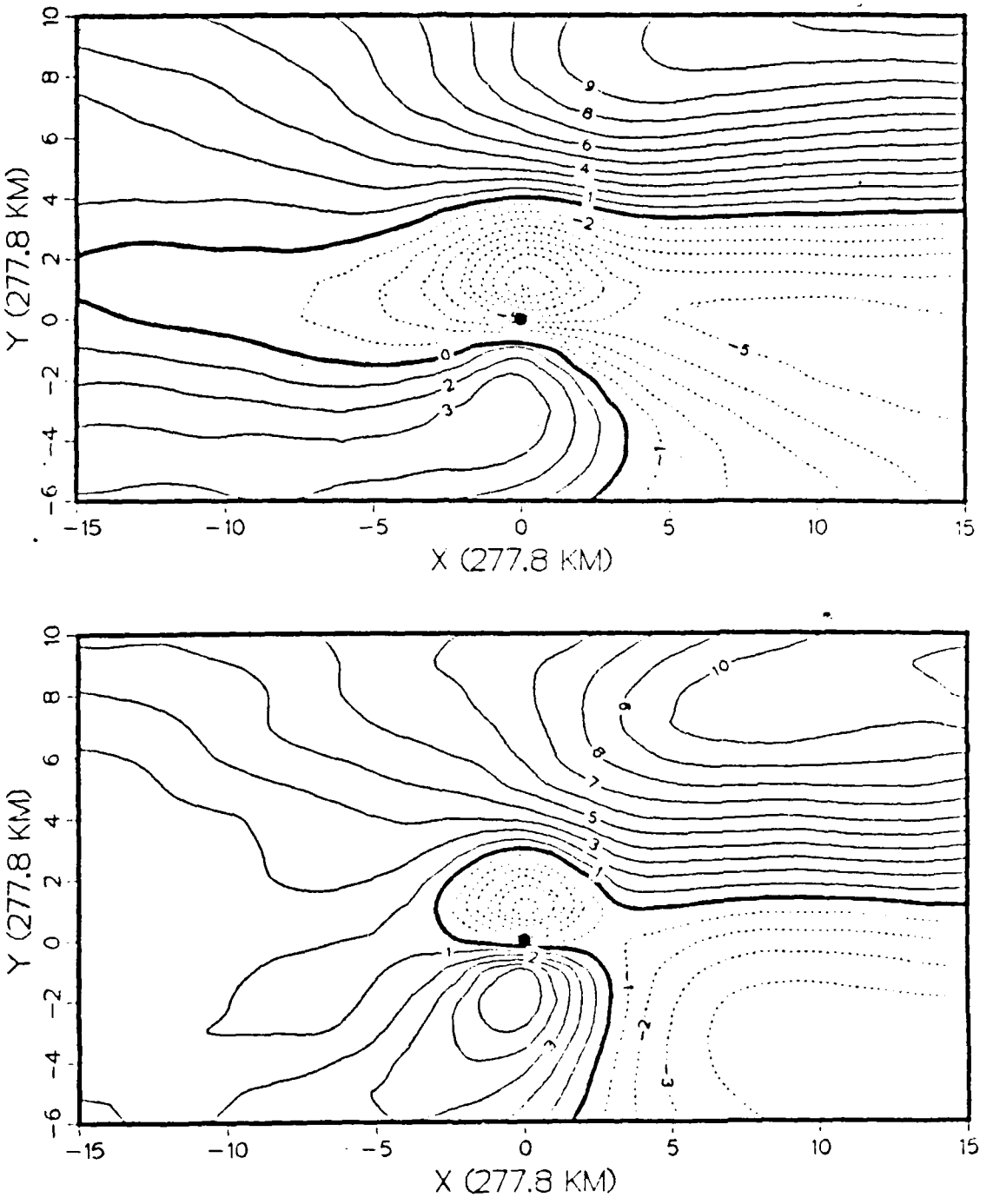

Fig. 3.1. The 700 mb zonal wind component composites using 35 EOF modes for Category 4 (top) and Category 5 (bottom). Westerly components (m/s) are positive (solid lines), while easterlies are negative (dotted lines). Solid thick line is zero m/s. Dot indicates vortex location.

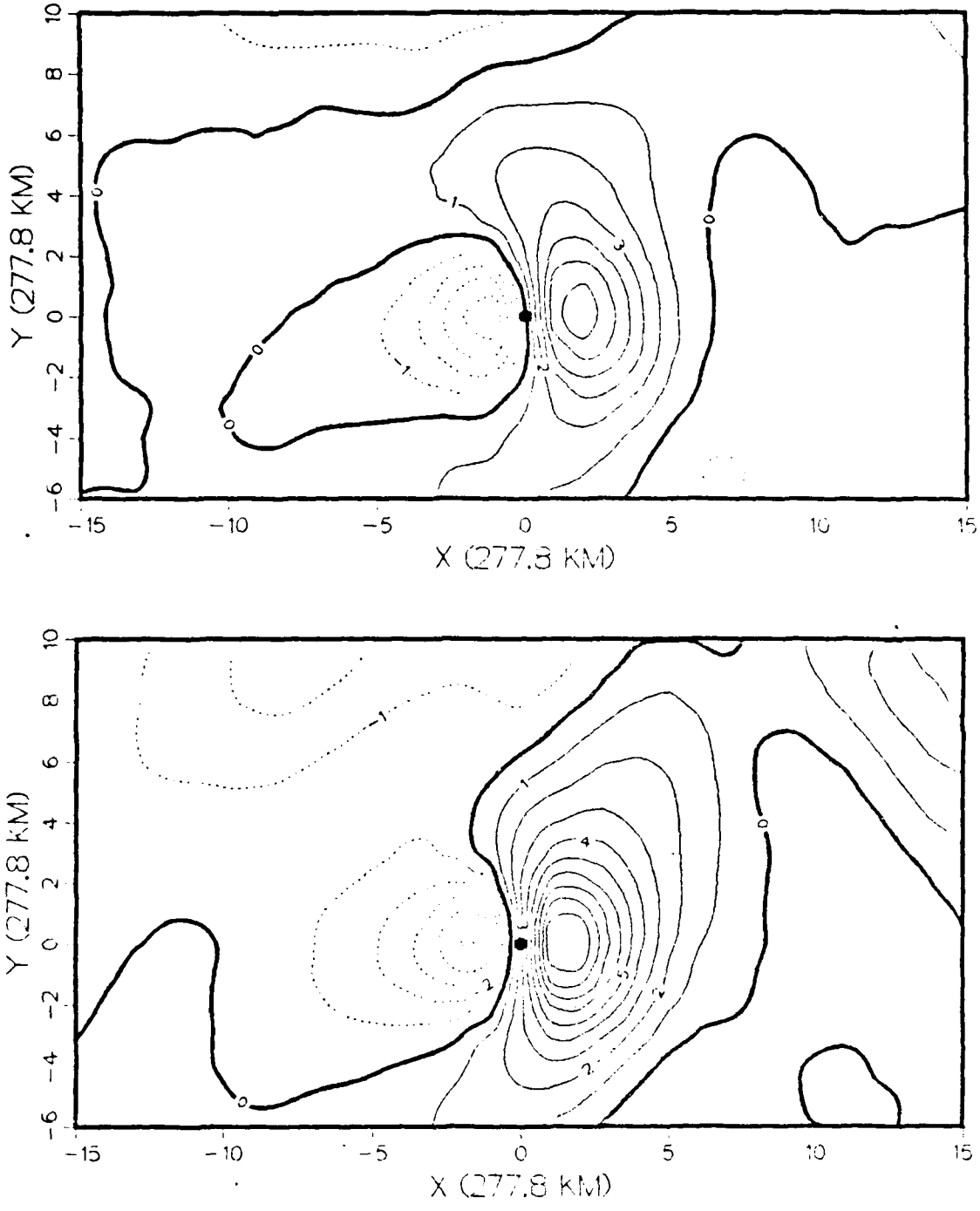

Fig. 3.2. The 700 mb meridional wind component for Category 4 (top) and Category 5 (bottom) using 35 EOF modes. Southerly components (m/s) are positive (solid lines), northerlies are negative (dotted lines), and solid thick line is zero m/s. Dot indicates vortex location.

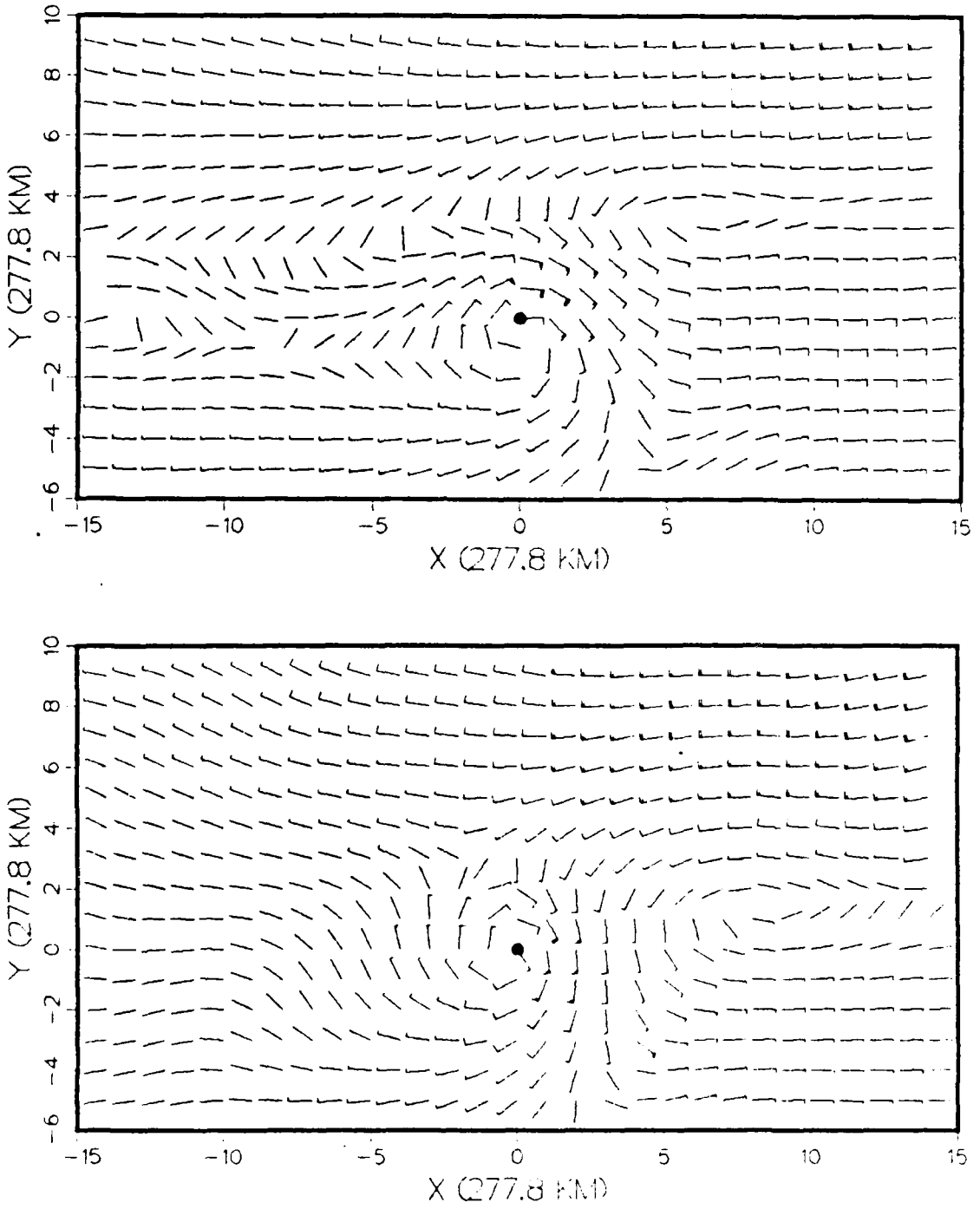

Fig. 3.3. The 700 mb vector wind composites using 35 EOF modes for Category 4 (top) and Category 5 (bottom). A pennant is 25 m/s, a barb is 5 m/s, and a half-barb is 2.5 m/s. Dot indicates vortex center.

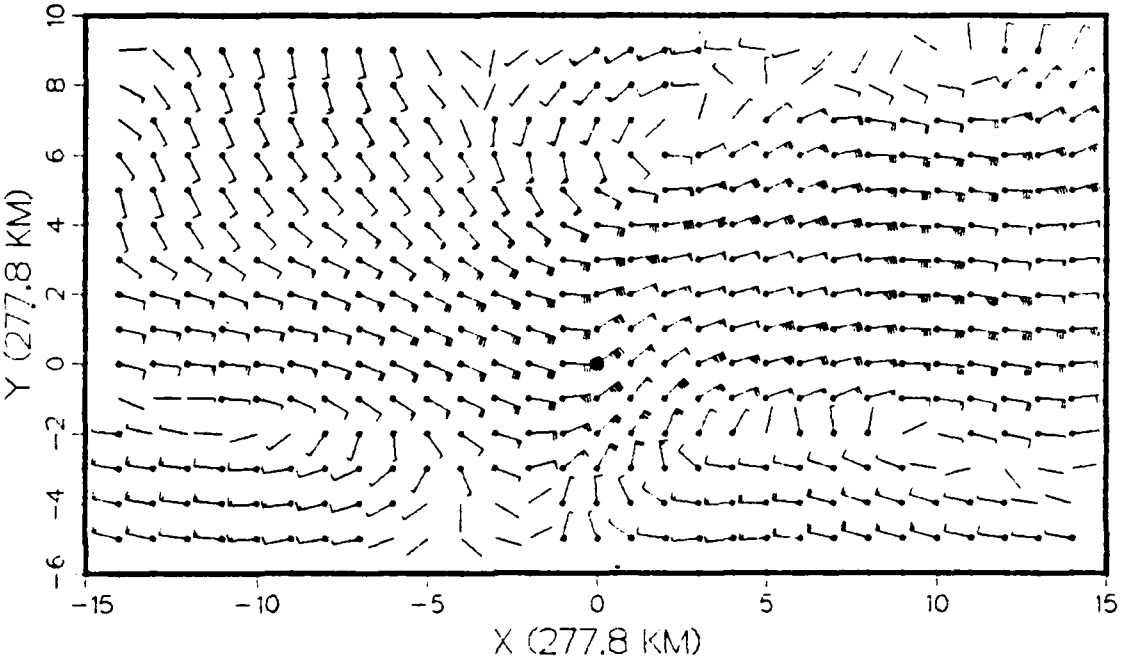

Fig. 3.4. The 700 mb wind difference field using Category 4 minus 5 based on 35 EOF modes. A pennant is 5 m/s, a barb is 1 m/s, and a half-barb is 0.5 m/s. If either the u or the v component difference is significantly different from zero (based on the Student's t-test with 95% confidence), a dot is plotted at the origin of the difference vector (a total of 433 significant points are plotted). Large dot indicates vortex location.

This strongly suggests that the synoptic forcing differs between the two categories.

The composite 400 mb u component fields (Fig. 3.5) reveal additional differences between the categories. In Category 5, the westerly components extend southward to the latitude of the vortex center, whereas a strong easterly component is found north of the vortex at 700mb. This indicates that the average cyclone found in this category experiences a vertical wind shear between 700 and 400 mb. Notice that the mean u component at 400 mb in Category 4 is again negative to the north of the vortex.

The 400 mb vector wind fields for Category 4 (Fig. 3.6) show the tropical cyclone as an open wave in the easterlies. Chan (1985) found a similar result from composites of the GBA winds for westward-moving cyclones. He pointed out that this could be partially explained by the lack of upper-air data in the vicinity of the tropical cyclone. Another reason may be the inadequacy of the grid resolution of the GBA to describe the smaller radial extent of the tropical cyclone at upper levels. Notice that the Category 5 wind field reveals a open wave in the westerlies. These contrasting features indicate that the vortex in each category is experiencing different synoptic forcing.

Many of the same features discussed above are also found at 250 mb. The zonal composites (not shown) have the vortex embedded in a belt of easterlies for Category 4 and westerlies for Category 5. As at the lower levels, the meridional wind composite (not shown) for Category 5 east of the vortex has a stronger southerly component than that found in Category 4. The total wind fields (not shown) have a closed anticyclone east of the vortex for both categories.

Composite fields for each of the five past-motion categories are made using 5, 10, 20 and 35 EOF modes. Category 4 (northwestward) will be used as a standard for

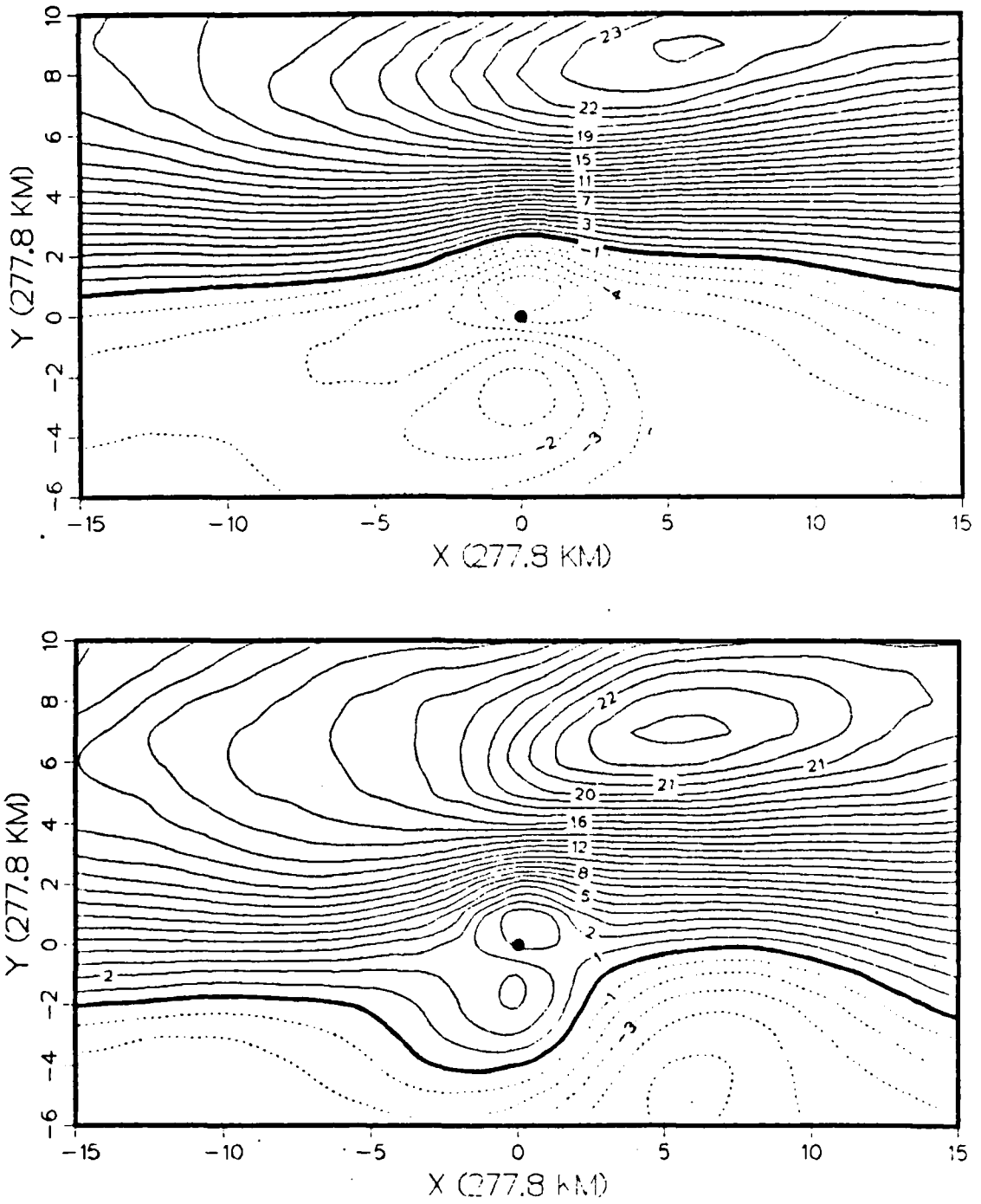

Fig. 3.5. As in Fig. 3.1, except for the 400 mb zonal wind composites for Category 4 (top) and Category 5 (bottom).

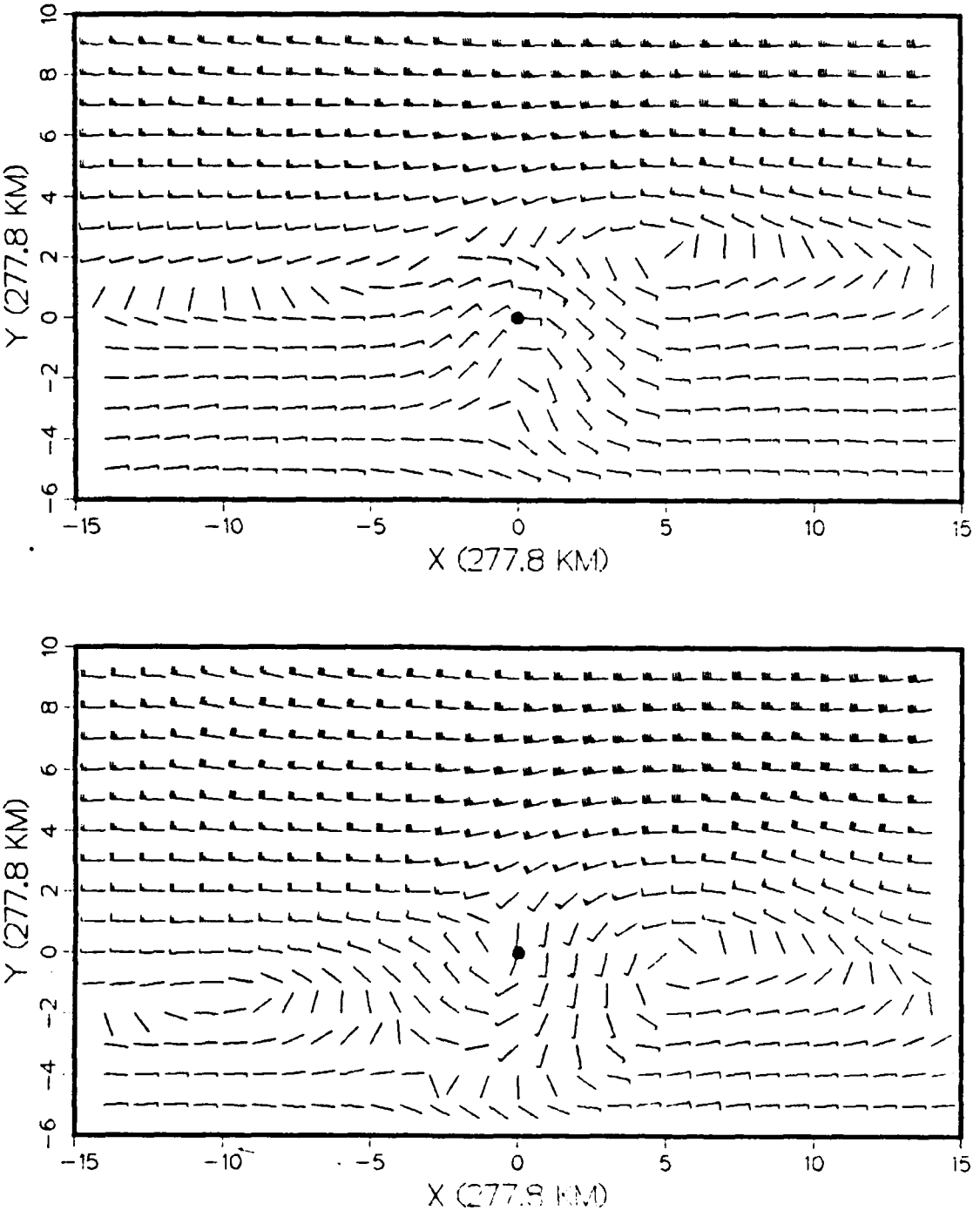

Fig. 3.6. As in Fig. 3.3, except for the 400 mb vector wind composites for Category 4 (top) and Category 5 (bottom).

comparison with the other categories because it contains the largest number of cases, and the overall mean movement of tropical cyclones in the western North Pacific is very similar to the mean movement in Category 4 (Chan, 1985). The past-motion categories 1, 2, 3 and 5 are each subtracted from Category 4 and the Student's t-test is performed at each gridpoint. Table 7 summarizes the total number of gridpoints for which the u or the v component is significantly different between the two categories being compared. The number of significant gridpoints varies from 96 to 491 out of a possible 527 points. The smallest number of significant points is generally found in the 4-1 category, while the largest number of significant points is generally found in the 4-5 category. Using 35 EOF coefficients for compositing, the differences in the 700 mb u component field between Categories 4 and 5 are significant at 355 of the 527 gridpoints. Similar results can be found in the other difference categories, although the number of gridpoints with significant differences is not as large. Based on the results of Table 7, a statistical basis exists for stating that the wind component fields for Categories 1, 2, 3 and 5 are different from those in Category 4.

Notice that the number of significant points generally decreases as the number of EOF modes in the composite increases. For example, the category 4-5 difference u composite fields at 700 mb decreases from 285 significant points for five modes to 229 significant points for 35 modes. The Student's t-test value is inversely proportional to the sum of the sample variances. Since more of the variance in the wind field is associated with 35 modes than with only five modes (Wilson, 1984), smaller t-values will be found. Thus, the chance of the wind components between the two categories being significantly different decreases with the inclusion of more EOF modes.

Table 7. Number of gridpoints for which the u or the v component for Categories 1, 2, 3 or 5 are significantly different from Category 4. The number of EOF modes used in the compositing is indicated inside the parentheses.

Level	Field	Cat	Number of EOF modes (5)	(10)	(20)	(35)
700	u	4-1	285	279	236	229
		4-2	378	366	334	302
		4-3	249	244	265	258
		4-5	427	391	364	355
	v	4-1	297	257	248	231
		4-2	358	299	239	226
		4-3	324	305	275	242
		4-5	342	290	280	281
400	u	4-1	220	191	169	168
		4-2	377	312	297	297
		4-3	299	260	291	267
		4-5	455	418	420	405
	v	4-1	327	278	265	247
		4-2	345	312	249	224
		4-3	341	283	234	213
		4-5	335	280	262	240
250	u	4-1	126	136	101	96
		4-2	428	381	351	350
		4-3	305	285	284	285
		4-5	491	466	455	458
	v	4-1	241	202	212	190
		4-2	356	315	288	269
		4-3	357	351	322	293
		4-5	347	276	284	252

For all the categories, the mean u and v component fields at all three levels (not shown) constructed using 5, 10, 20 or 35 EOF modes reveal only minor differences. The magnitude of the wind vectors in the five-mode EOF wind composites are slightly smaller than those in the 35-mode EOF composites. This is because more of the variance in the signal is defined when using 35 EOF modes (Wilson, 1984). Another minor difference is in the wind direction for light winds (less than 5 m/s). This does not indicate that reconstruction of a u field for a particular case can be done with only five EOF eigenvectors. Wilson (1984) shows

that the first 35 eigenvectors contain signal. However, the patterns produced in a component field by the 6-35 eigenvectors are not consistently in the same position relative to the vortex. Therefore, these features are smoothed during compositing.

B. TERCILE PATTERN COMPOSITES

As mentioned in Chapter 2, each of the five past-motion categories can be divided into tercile subcategories based on either the AT or CT component with respect to CLIPER at each forecast interval (24, 48 and 72 h). By comparing the composite wind fields of these tercile subcategories, it is possible to evaluate further the suitablility of using wind-based EOF analysis to define "synopticity" (i.e., basic synoptic patterns affecting cyclone motion). Examples of the Category 4 storm tracks in the Left, Center and Right subcategories are plotted in Fig. 3.7. Category 4 is chosen because it has the largest sample size. The track plots show a reduction in the scatter of the 72-h positions compared with the overall Category 4 tracks in Fig. 2.5. As might be expected, storms in the Left subcategory show a strong westward zonal displacement. In contrast, the Right subcategory has the majority of recurving cases.

Composite u and v fields are calculated separately for storms within the tercile subcategories defined by the CT72 components. Pairs of tercile subcategory fields are subtracted and at each grid point a Student's t-test is used to determine if the tercile composite fields are significantly different at the 95% confidence level. A summary of the test results is found in Table 8. The smallest number of significant points is generally found in the Left minus Center category. The 400 and 250 mb fields are very similar based on these comparisons. Notice that in the Left minus Center category the number of significant points decreases with elevation, whereas this number

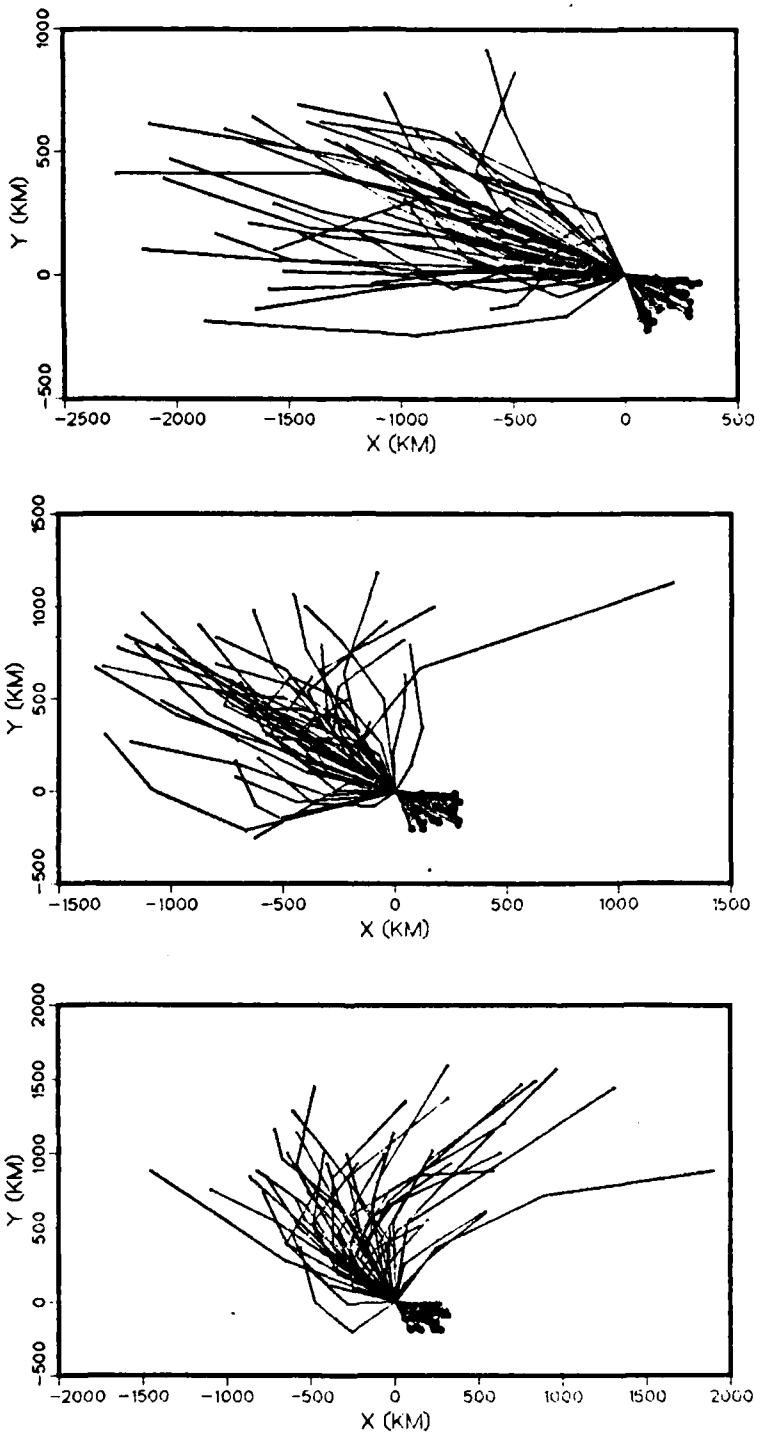

Fig. 3.7. As in Fig. 2.4, except the 50 storm tracks are from Category 4 storms in tercile subcategories Left (top), Center (middle) and Right (bottom).

increases with elevation in the Center minus Right category. This latter feature would indicate that differences in the environmental flow between storms moving along a CLIPER track and those moving to the right of a CLIPER track are more significant at the upper levels than at the lower levels. Over half of the grid points (282 points) have significantly different 700 mb u components for the Left minus Right comparison. Since the largest differences appear in the Left minus Right comparison, these composite fields are chosen for further study. The composite fields will be examined to determine if the synoptic patterns differ between the subcategories. That is, can the current synoptic patterns be related to the 72-h cyclone position relative to a CLIPER reference?

Table 8. As in Table 7, except the number of gridpoints at which the wind components are significantly different is computed between two CT72 terciles of Category 4 storms.

		CT72 Tercile Difference Fields		
Level	Field	Left-Center	Left-Right	Center-Right
700	u	178	282	123
	v	126	150	44
400	u	94	259	107
	v	33	120	48
250	u	72	256	149
	v	36	121	56

The 700 mb mean u fields for the CT72 Left and Right tercile subcategories (Fig. 3.8) appear to be very similar to that for the overall Category 4 sample (Fig. 3.1). However, the extent and magnitude of the easterlies north of the vortex in the Left subcategory are larger than those in the Right subcategory. This is consistent with the Left subcategory storms having a stronger westward component of

motion. The mean v component fields have a stronger southerly component to the east of the vortex in the Right tercile category (Fig. 3.9). This feature appears in the composite total wind fields as a strong confluence band to the southeast of the vortex in the Right category (Fig. 3.10). When the two mean wind fields are subtracted (Fig. 3.11), areas with significantly different forcing become apparent. The largest differences are found to the east of the vortex, which indicates that the convergence band and the anticyclone to the northeast of the vortex play an important role in the motion of the cyclones within these two subcategories. The composite wind fields at 400 and 250 mb (Figs. 3.12 and 3.13) show a more intense anticyclone to the northeast of the vortex in the Right subcategory than in the Left subcategory. The anticyclone to the west of the vortex for the Right subcategory is well defined at 400 mb, which suggests a break in the ridge, and hence possible recurvature.

Another demonstration that the EOF analysis can be used to define synopticity can be made by studying the composite wind fields defined within terciles of the AT72 component. The AT72 tercile divisions are defined as Slow, Center and Fast with respect to the CLIPER forecast. Fifty storm tracks for the AT72 subcategories are shown in Fig. 3.14. Notice that the Fast subcategory isolates most of the storm tracks that translated the greatest distances in the 48-h to 72-h interval. The Slow subcategory appears to have a large number of storms that continued to move northwestward at slow speeds. However, there are a few storms that moved left or right of a northwest track. These large deviations arise because the CLIPER forecast positions at 60 and 72 h vary with each individual storm based on persistence and initial storm parameters.

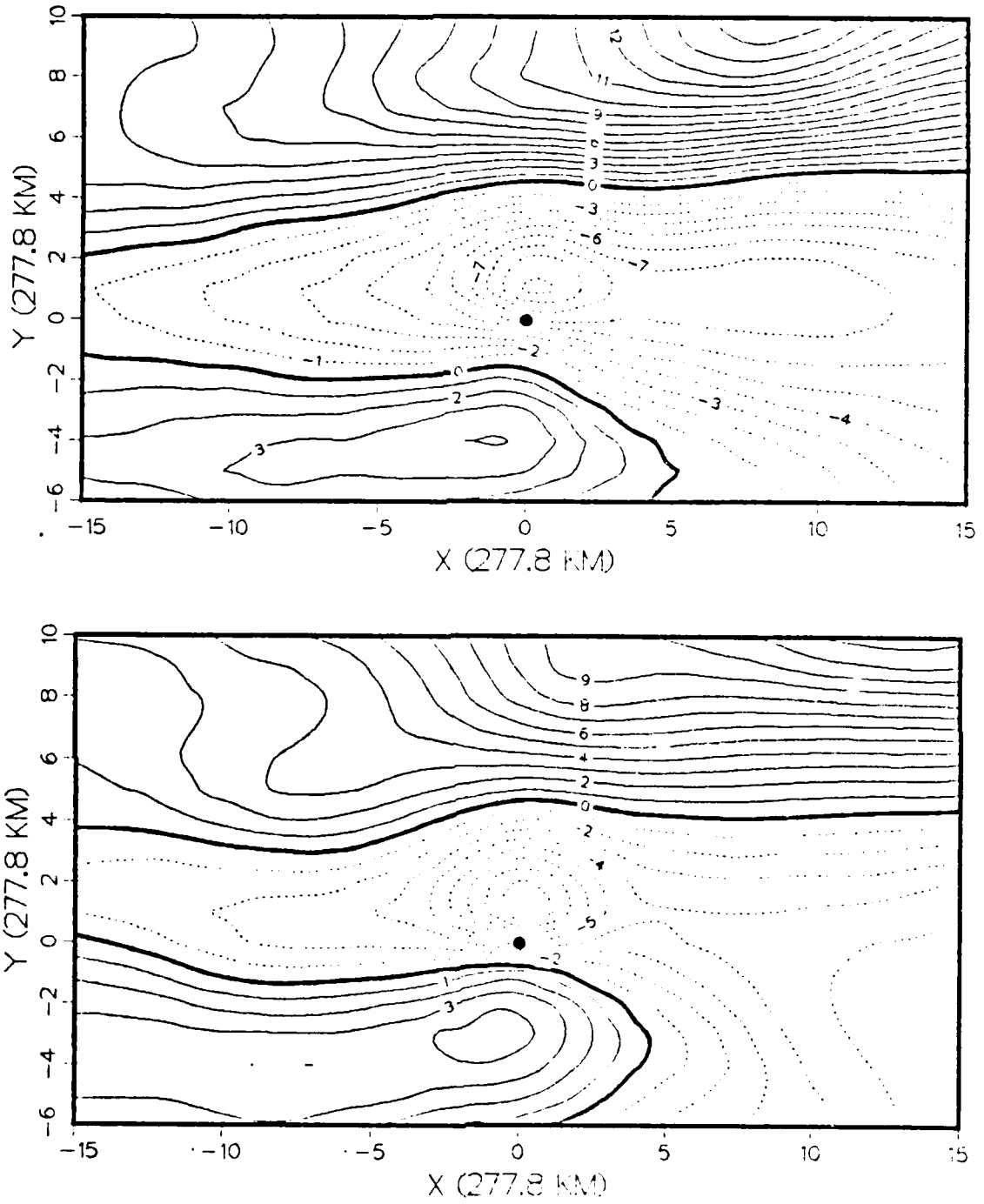

Fig. 3.8. As in Fig. 3.1, except for the 700 mb mb zonal wind composites in Category 4 CT72 Left (top) and Right (bottom) subcategories. The composites were made using 35 EOF modes.

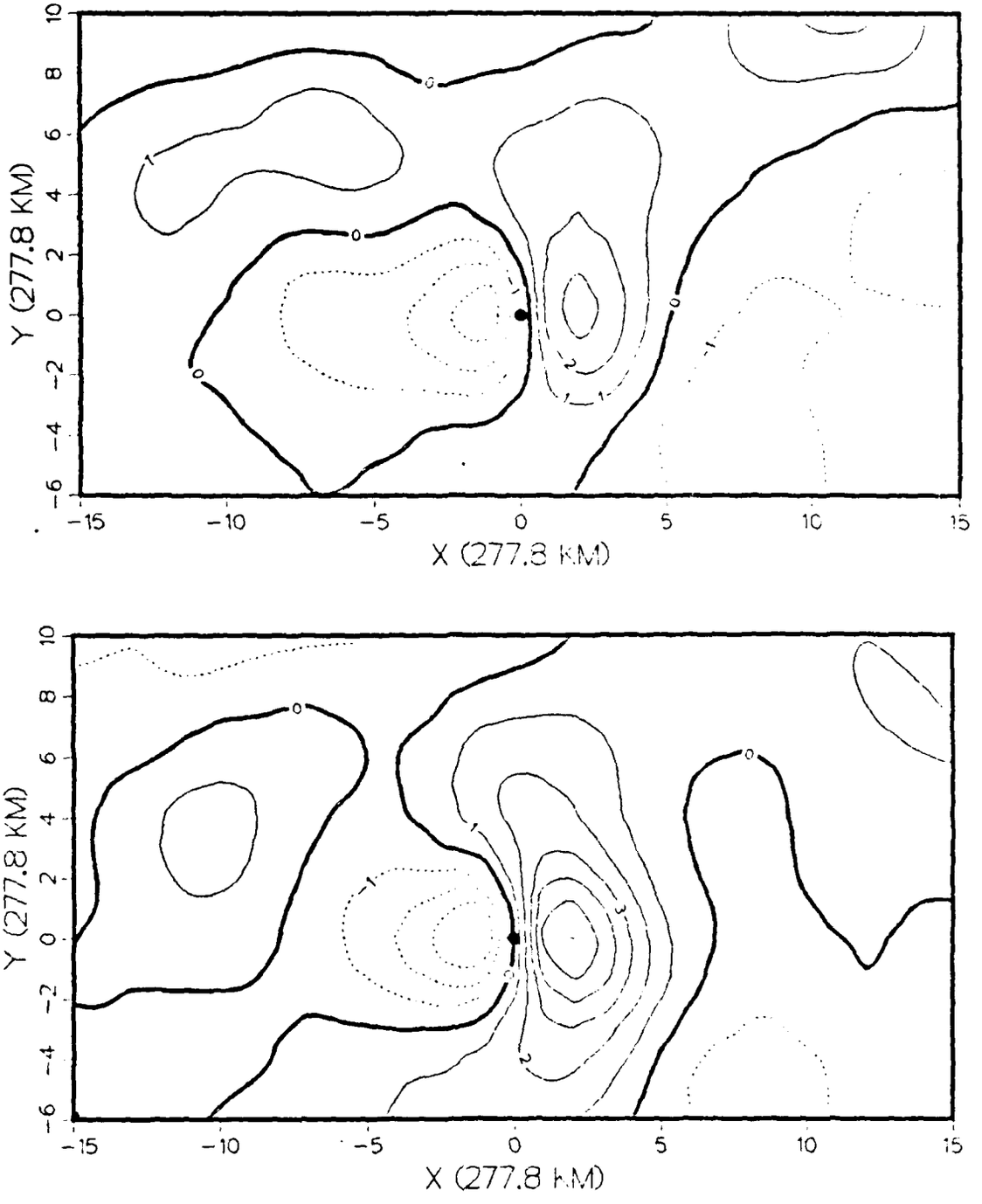

Fig. 3.9. As in Fig. 3.2, except for the 700 mb meridional wind composites in the Category 4 CT72 Left (top) and Right (bottom) tercile subcategories.

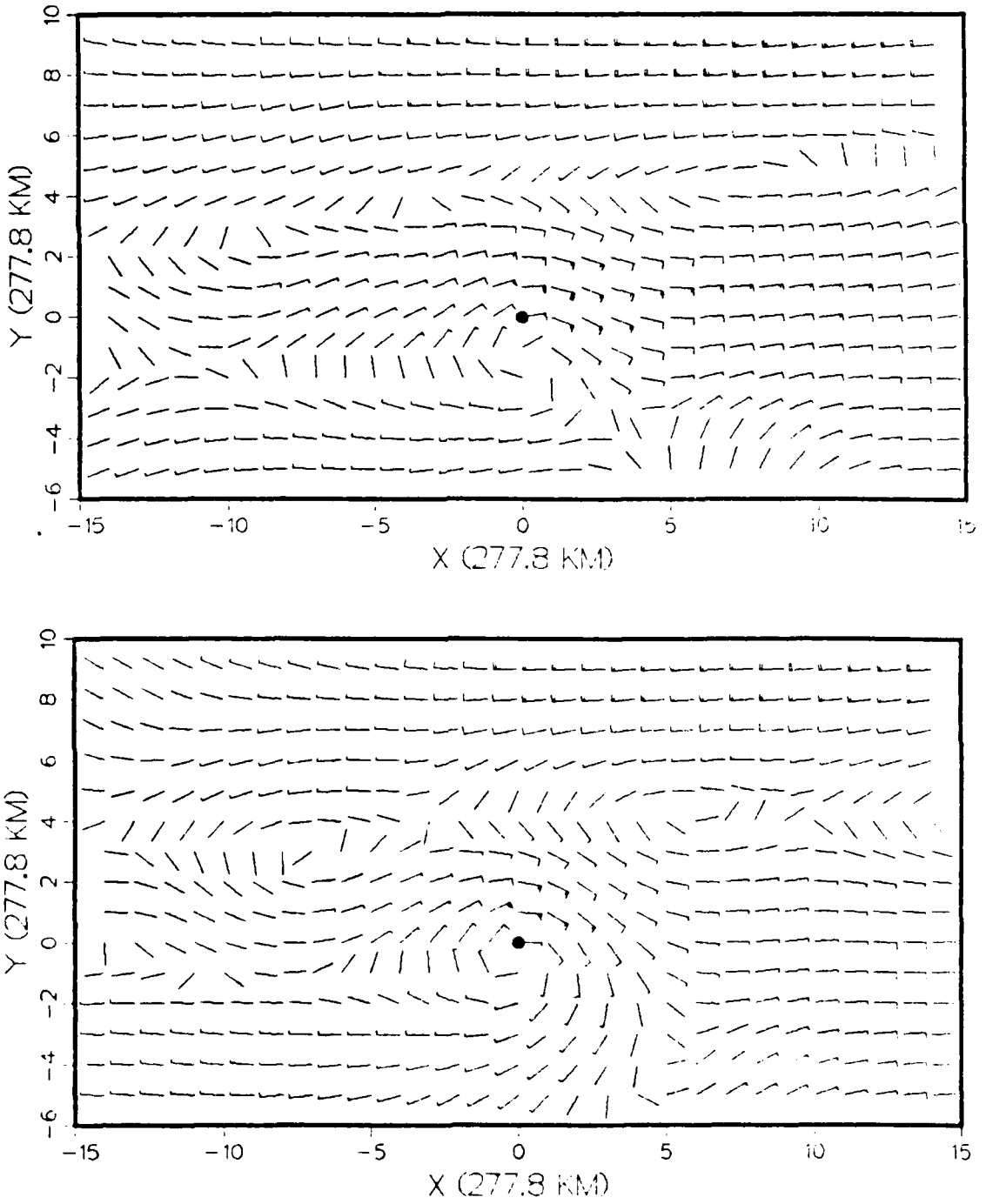

Fig. 3.10. As in Fig. 3.3, except for the 700 mb vector wind composites for Category 4 CT72 Left (top) and Right (bottom) subcategories.

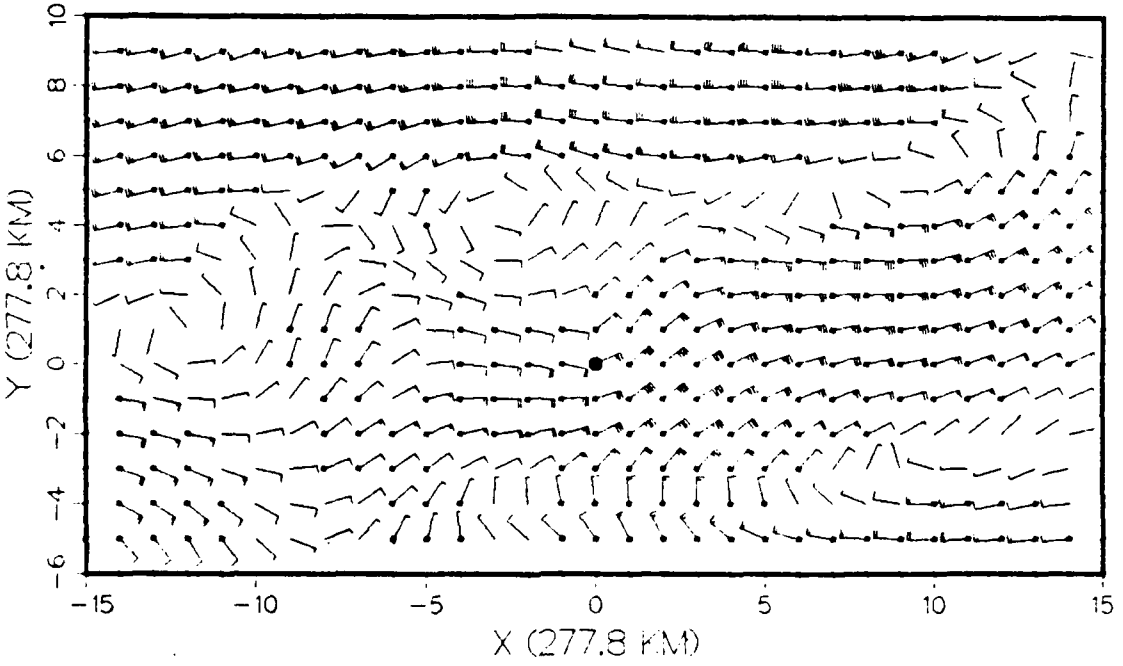

Fig. 3.11. As in Fig 3.4, except using Category 4 Left minus Right terciles (347 significant points are plotted).

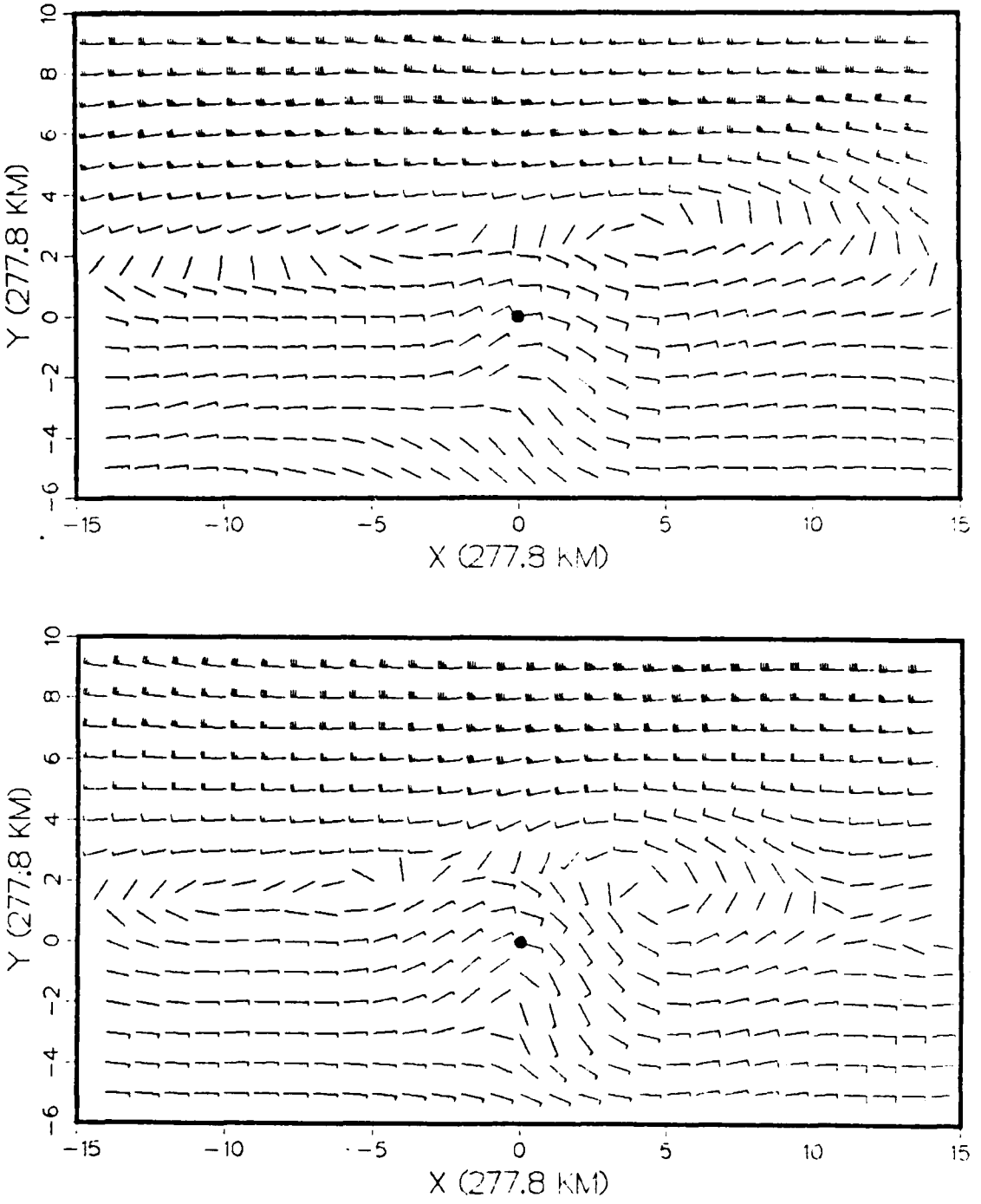

Fig. 3.12. As in Fig. 3.3, except for the wind composites at 400 mb in the CT72 Left (top) and Right (bottom) subcategories.

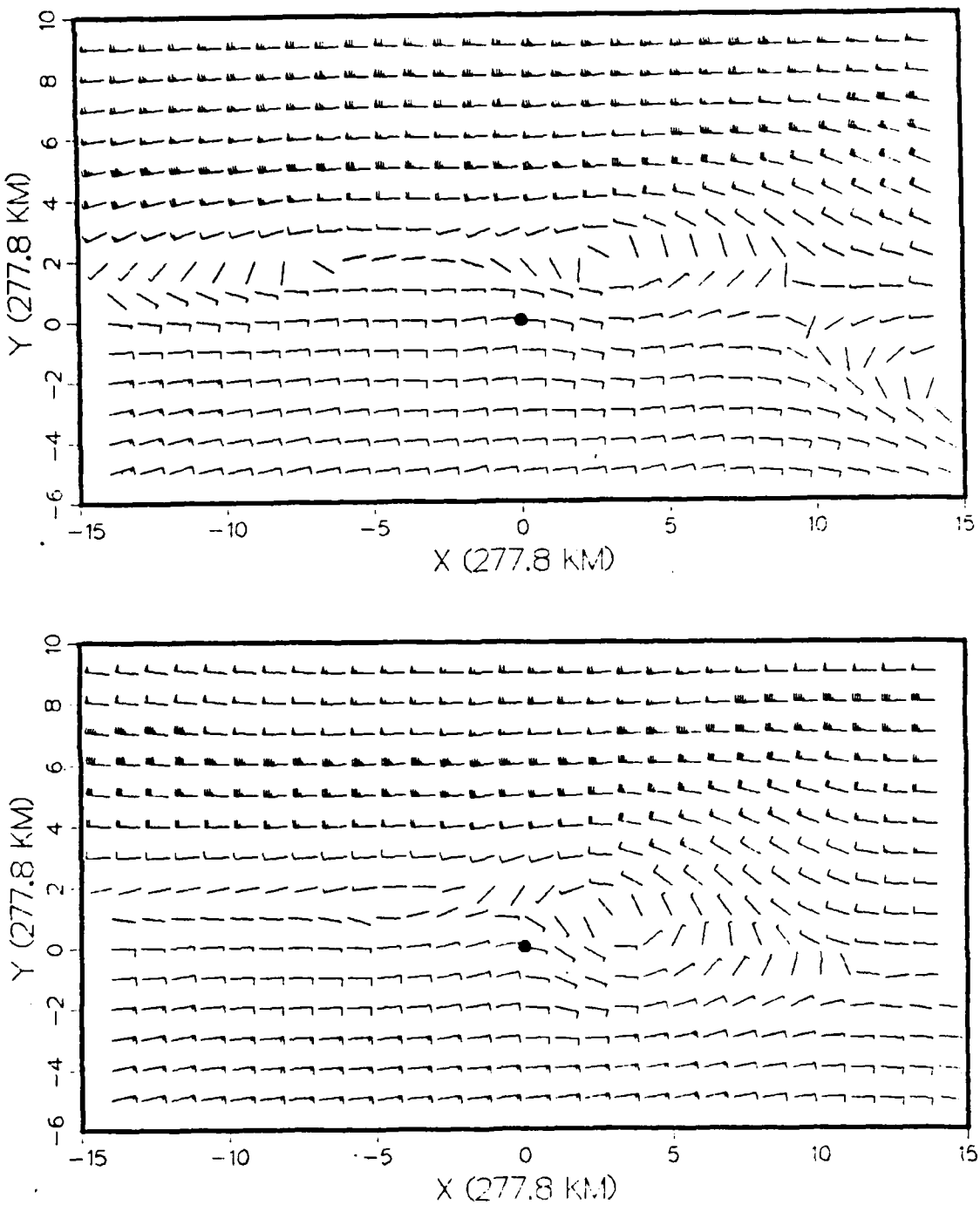

Fig. 3.13. As in Fig. 3.3, except for 250 mb wind composites in the CT72 Left (top) and Right subcategories (bottom).

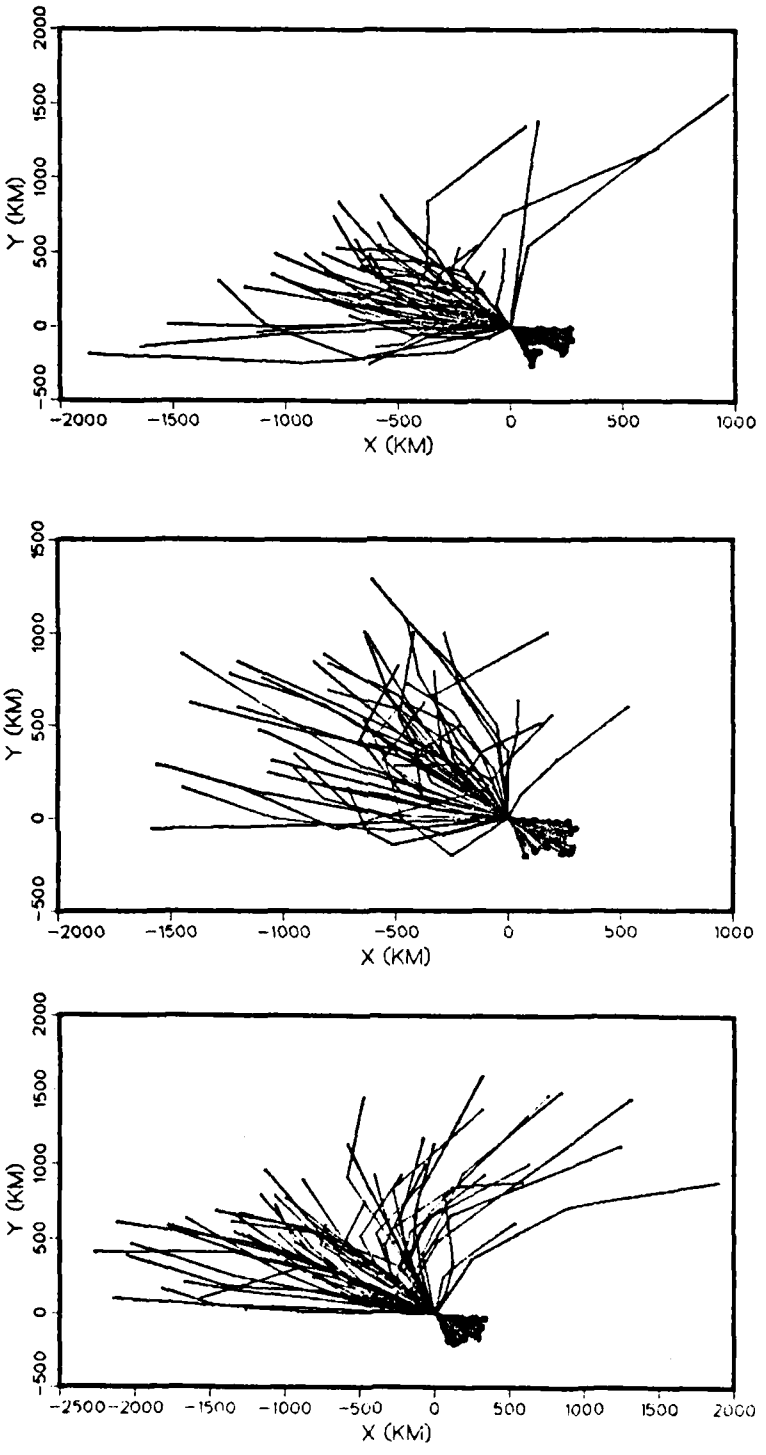

Fig. 3.14, As in Fig. 2.4, except for 50 storm tracks from Category 4 storms in the Slow (top), Center (middle) and Fast (bottom) subcategories.

As before, composite u and v fields are calculated for each of the tercile subcategories (Slow, Center and Fast) defined by the AT72 components. The u or the v composite fields are subtracted and at each gridpoint a Student's t-test is used to determine if the tercile composite fields are significantly different (Table 9). The smallest number of significant points is found in the Center minus Fast subcategory. The number of significant points decreases from 700 to 400 mb in the mean u fields and increases from 700 to 400 mb in the mean v fields. This indicates that the zonal EOF modes at 700 mb should better define the differences within these categories and the meridional EOF modes at 400 mb should better define the differences within these categories. In general, the number of significant points is smaller for the AT72 tercile comparisons than is found in the CT72 comparisons (Table 8). This suggests that less information content exists in the EOF wind components regarding the AT72 track components than for the CT72 track components. Because the largest differences in composite fields are in the Slow minus Fast comparisons, these two subcategories are chosen for further study.

Table 9. As in Table 7, except the number of gridpoints at which the wind components are significantly different are for the AT72 tercile difference comparisons.

		AT72 Tercile Difference Fields		
Level	Field	Slow-Center	Slow-Fast	Center-Fast
700	u	140	137	55
	v	94	112	6
400	u	77	87	14
	v	115	122	49
250	u	169	169	35
	v	107	123	65

The composite zonal fields at 700 mb have a stronger meridional gradient in the vortex region for the Fast subcategory (Fig. 3.15) than for the Slow subcategory. The zonal gradient of the meridional wind composite fields across the vortex is also larger in the Fast subcategory (Fig. 3.16). Notice the stronger southerly component east of the vortex in the Fast subcategory. These trends indicate that the total winds are stronger within the vortex region in the Fast subcategory. These synoptic features at 700 mb are well defined in the composite wind fields (Fig. 3.17). The extent of the cyclonic circulation is larger in the Fast subcategory. Notice also that the anticyclone to the northeast is more organized and much closer to the vortex in the Fast subcategory. When the wind fields at 700 mb are subtracted (not shown), the largest differences (3 m/s) are found west of the vortex.

Even larger synoptic differences are found at the upper levels. The total 400 mb wind composites (Fig. 3.18) indicate a more pronounced wave in the easterlies near the vortex for the Fast subcategory. The wind difference plots at 400 and 250 mb are shown in Fig. 3.19. As expected from Table 9, the meridional component accounts for the majority of the significant points plotted at 400 mb. That is, those wind barbs with significant differences show a more north-south orientation. However, the zonal and meridional component differences at 250 mb are important in different areas. The meridional component tends to be more significant in the northern portion of the grid, while the zonal component is significant southwest and east of the vortex.

In summary, the composite analysis has demonstrated that the EOF modes can be used to describe statistically significant differences in the mean wind fields. The synoptic forcing is clearly different between Categories 4

and 5, and this forcing is consistent with the mean motion of these categories. The same synoptic features are evident in the mean wind composites using five and 35 EOF modes. Storms in the Left and Right CT72 terciles within Category 4 are also associated with different synoptic patterns. Although the composite patterns in the terciles resemble those derived for Category 4, there are noticeable differences. Similarly, storms in the Slow and Fast AT72 terciles within Category 4 are found to be embedded in different synoptic flow patterns. Therefore, the truncated EOF coefficients contain synoptic information necessary to explain a large part of the future motion of the cyclones.

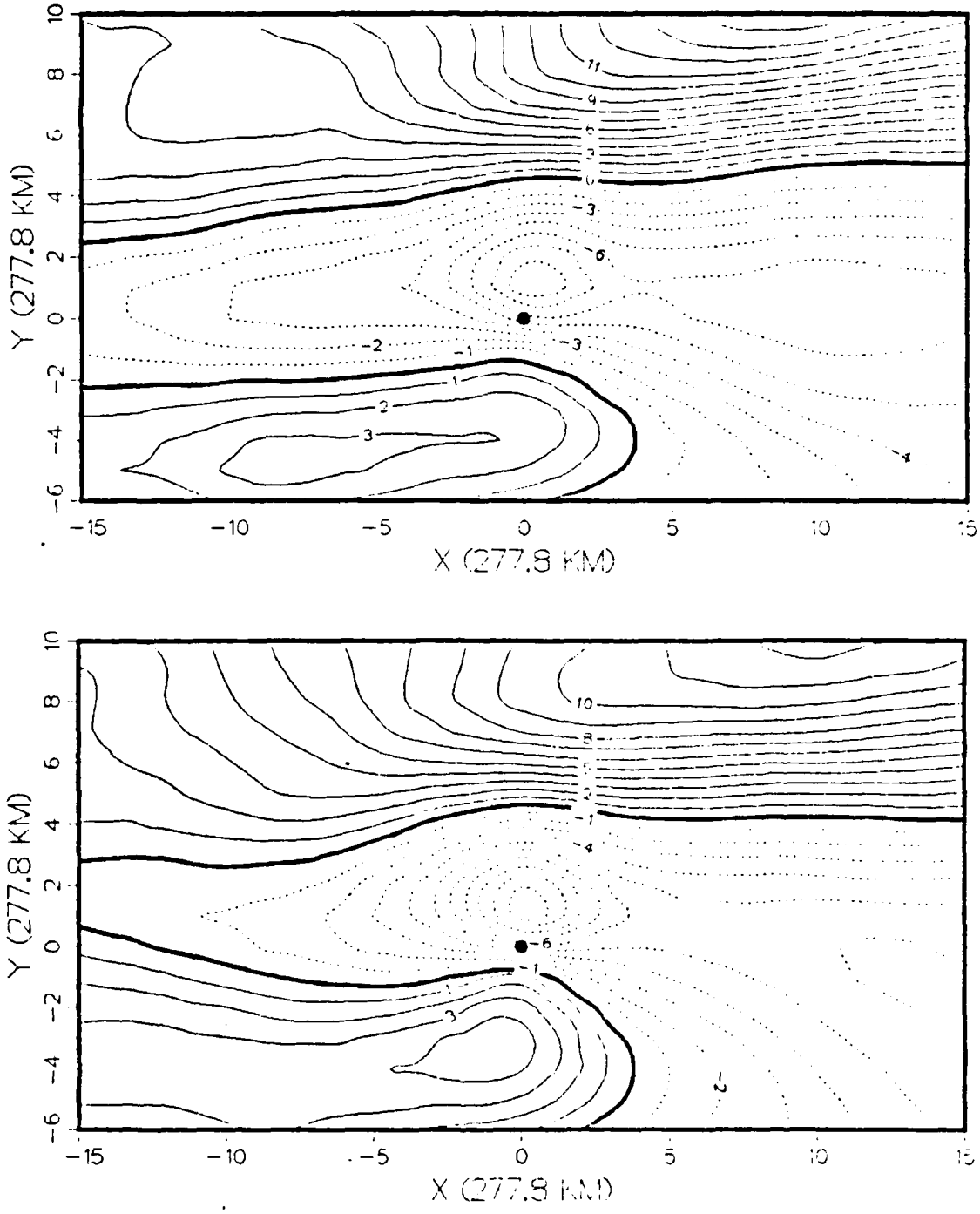

Fig. 3.15. As in Fig. 3.1, except for the zonal wind composites at 700 mb for the Category 4 AT72 Slow (top) and Fast (bottom) subcategories.

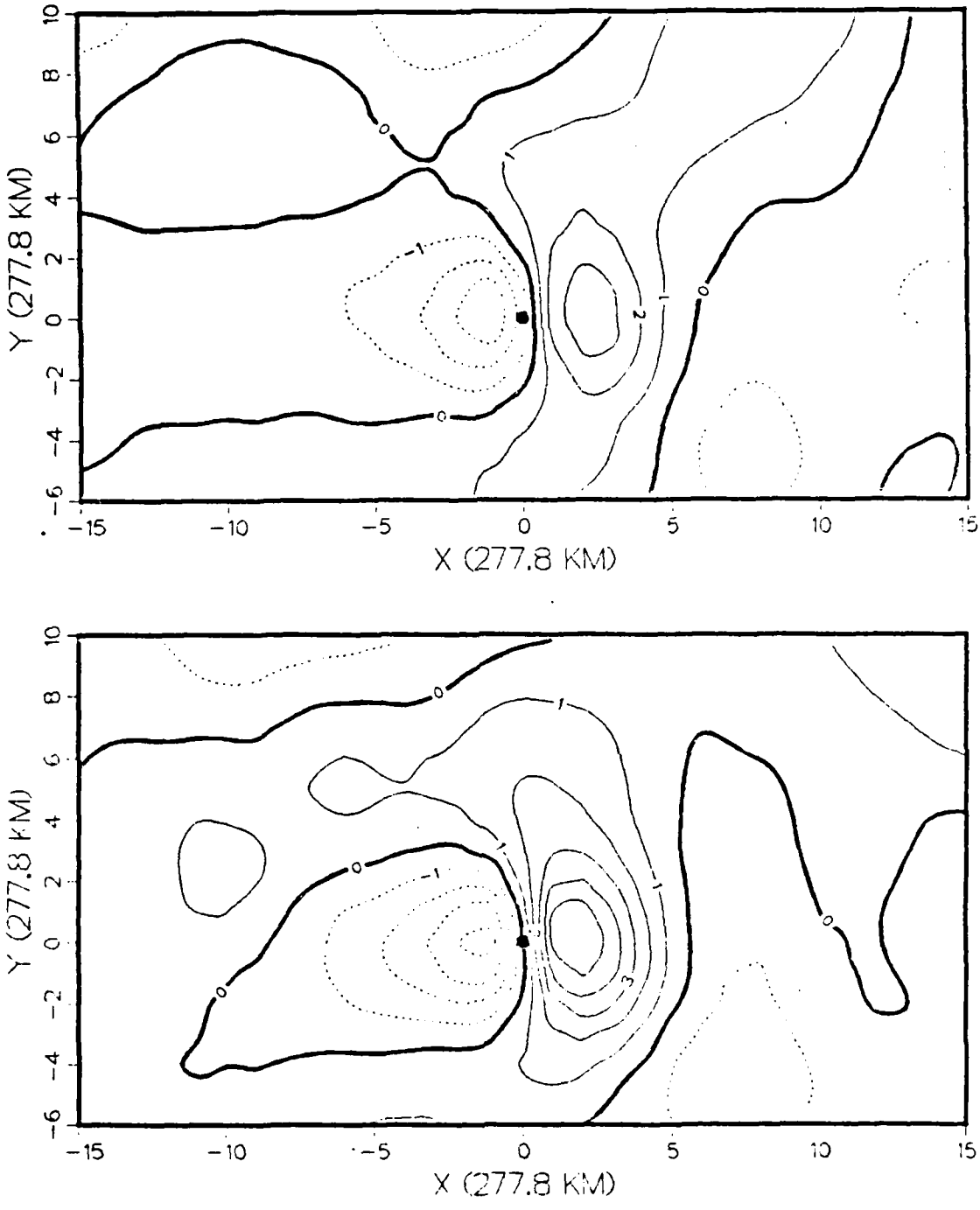

Fig. 3.16. As in Fig. 3.2, except for the meridional wind composites at 700 mb for the Category 4 AT72 Slow (top) and Fast (bottom) subcategories.

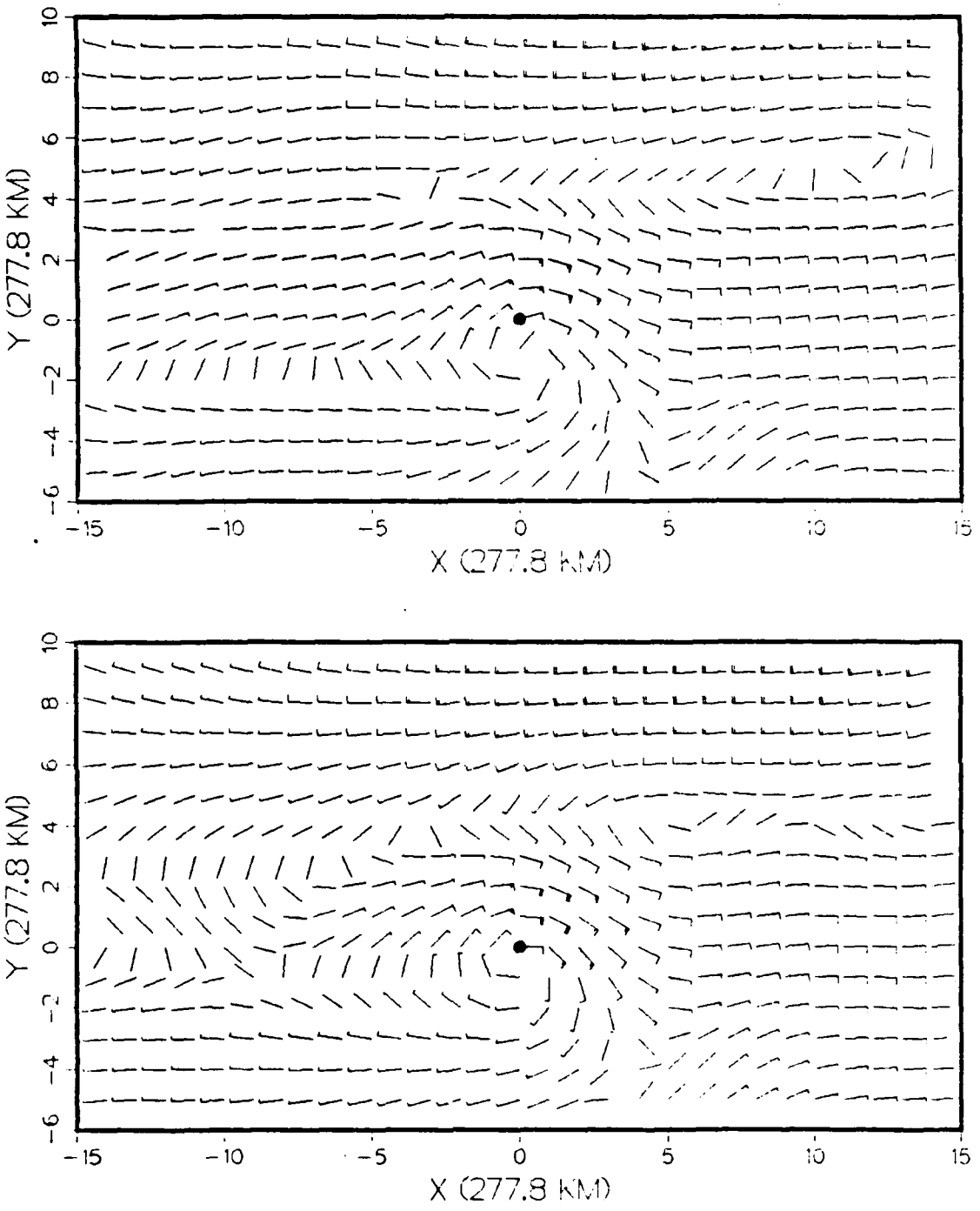

Fig. 3.17. As in Fig. 3.3, except for the 700 mb total wind composites for the Category 4 AT72 Slow (top) and Fast (bottom) subcategories.

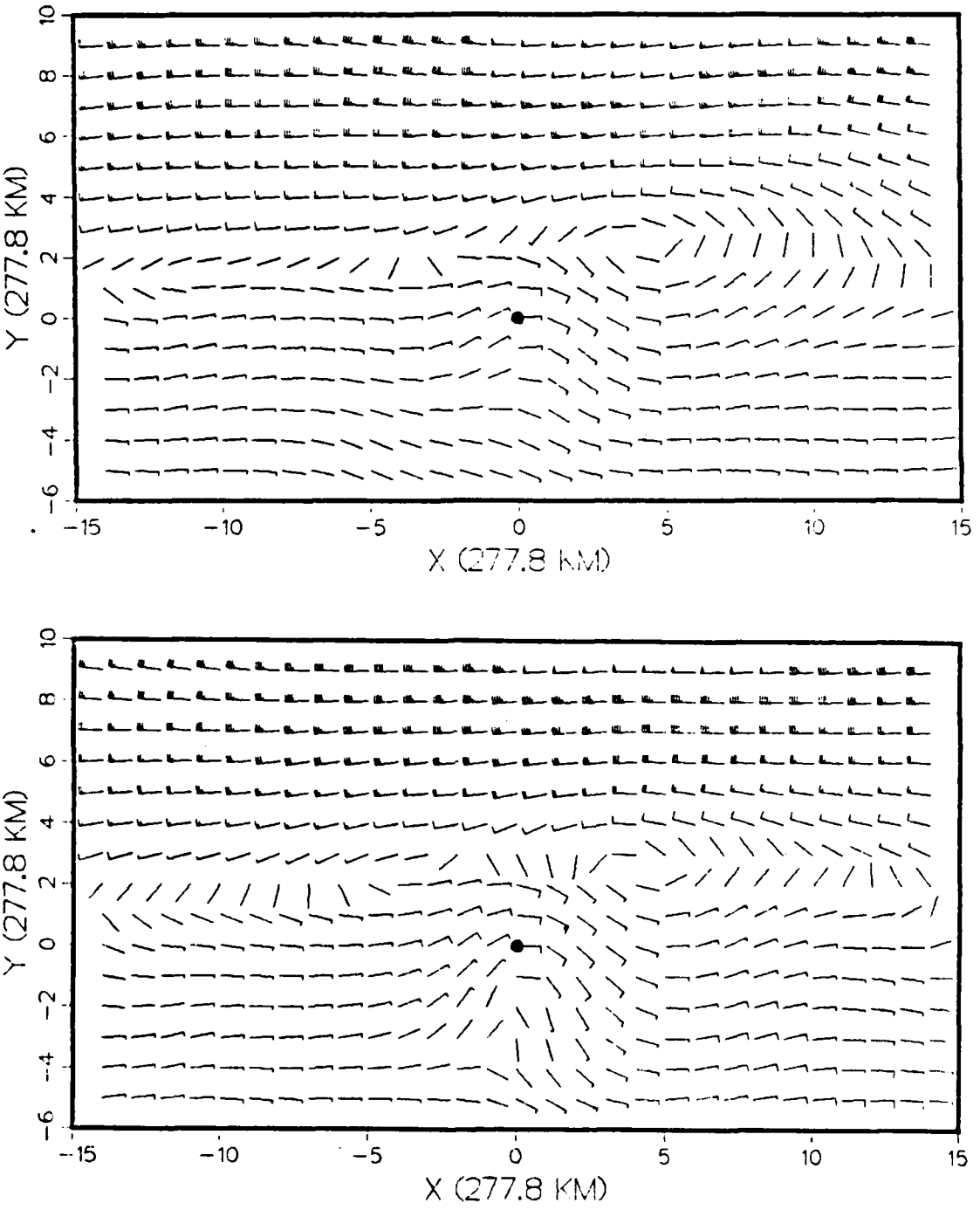

Fig. 3.18. As in Fig. 3.3, except for the 400 mb wind composite for the Category 4 AT72 Slow (top) and Fast (bottom) subcategories.

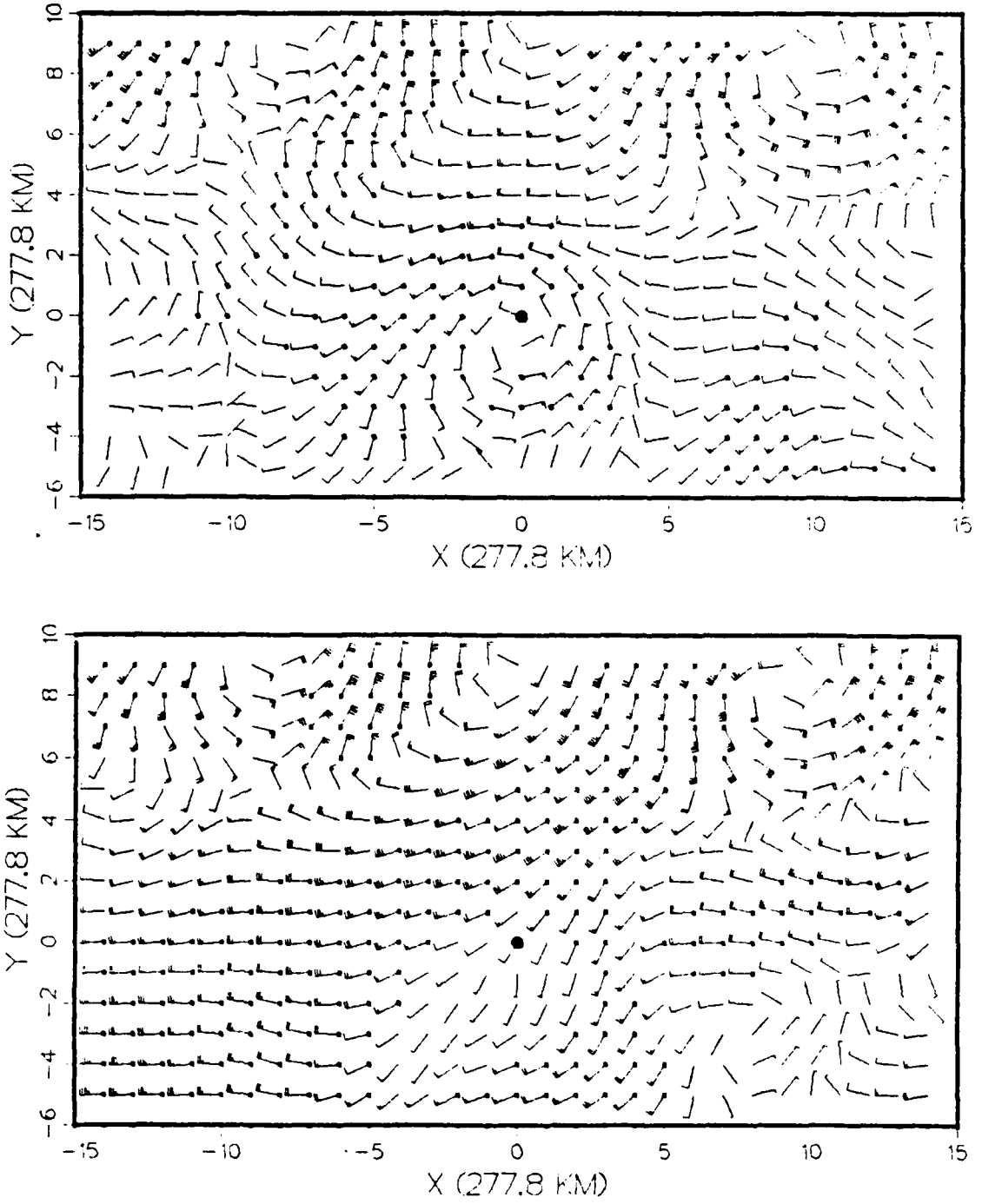

Fig. 3.19. As in Fig. 3.4, except for the wind difference composites Slow minus Fast at 400 mb (top) and at 250 mb (bottom).

IV. POST-PROCESSING THE OTCM FORECAST TRACKS

A. MOTIVATION

In prior studies on the performance characteristics of the JTWC objective forecast aids, the One-Way Tropical Cyclone Model (OTCM) has proven to be one of the best objective aids. Tsui (1984) evaluated the performance of 11 objective aids for western North Pacific tropical cyclones during 1979-1982. The OTCM had the lowest mean speed and forecast errors, and was second best in track error (see Chapter 1, section C for definitions). Elsberry and Peak (1986) evaluated the performance of nine forecast aids in terms of the CT/AT components relative to a persistence track defined by past 12-h movement. Both the CT and AT component samples were divided into tercile subcategories. The nine forecast aids were evaluated on how well they predicted the observed tercile subcategory at each forecast interval. In their study, the OTCM was classified as one of the top performing aids used by JTWC.

The forecast philosophy that has developed at JTWC is consistent with the results of these studies. Since the OTCM has demonstrated consistent skill in identifying track and speed changes, the OTCM forecast is used as the primary guidance for determining the future track of a tropical cyclone (Sandgathe, 1985). The OTCM forecast position at 72 h is modified in certain forecast scenarios based on other objective techniques and known model weaknesses. Two examples of modification to the OTCM include adjusting for a slow bias on post-recurvature tropical cyclones, and anticipating a more rapid response by the cyclone to midlatitude forcing than is indicated by the OTCM during recurvature situations.

An objective of this study is to develop and test a post-processing scheme for correcting the OTCM forecast track positions based on the synoptic forcing represented by the wind-based EOFs. The technique, to be discussed later, should help the JTWC forecaster recognize when the OTCM forecast positions need modification. The emphasis here is on the OTCM since it has already proven to be a valuable forecast aid.

B. MODEL DESCRIPTION AND DATA AQUISITION

The current version of OTCM is basically the model described by Hodur and Burk (1978). It is a single-grid, three-layer, primitive equation model. The coarse grid resolution is 205 km. The lateral boundaries have a one-way influence from the FNOC global model (Fiorino, 1985). The tropical cyclone is initially defined in the model as a vorticity bogus. Since the model is dry, the vortex circulation is maintained by a specified analytical heating function. Since no frictional or other physical processes are included, this model is mainly an advective model. Modifications to the 1978 version of the model include a new method for locating the model grid relative to the initial storm position and a stronger storm bogus. A pre-processing technique developed by Shewchuk and Elsberry (1978) has also been added. The technique (to be discussed later) adds a persistence component of motion in the model forecast track.

The OTCM forecasts from 1979-1983 were provided by T. Tsui of the Naval Environmental Prediction Research Facility. The 24, 48 and 72-h OTCM forecast positions are available at 00, 06, 12 and 18 GMT. The official forecasts from JTWC are also available, although not for every time the OTCM is run.

C. OTCM CT AND AT COMPONENTS

The CT and AT components of the OTCM forecasts are calculated relative to a CLIPER forecast track as described in Chapter 2 (Fig. 2.2). A statistical summary of the CT/AT components for the OTCM is shown in Table 10. Notice that the mean CT components at 48 and 72 h are negative. That is, the average OTCM forecast is to the left of the CLIPER forecast positions at these times. The negative mean AT components indicate that the average OTCM forecast positions are behind those of CLIPER.

Table 10. Mean ($\bar{X}$) and standard deviations (σ) of CT and AT components (km) for the OTCM forecasts during 1979-1983 (N = sample size). The CT and AT components are calculated with respect to a CLIPER track.

		CT		AT	
Time	N	$\bar{X}$	σ	$\bar{X}$	σ
24	1136	13	154	-126	189
48	1101	-24	341	-167	543
72	984	-108	522	-152	596

The frequency distribution of cases defined by the CT and AT components at 72 h is displayed in Fig. 4.1. Notice that the CT72 distribution is slightly skewed to the left, which indicates that the OTCM has a slight tendency to be left of a CLIPER forecast at 72 h. It is somewhat surprising to find AT components as negative as -3000 km. This situation could occur when the OTCM predicts recurvature and the CLIPER forecast is for a continuation toward the north. As before, the sample at each forecast interval can be divided into CT and AT tercile subcategories. For example, the Left subcategory at 72 h includes all storms with CT components that are smaller than -307 km.

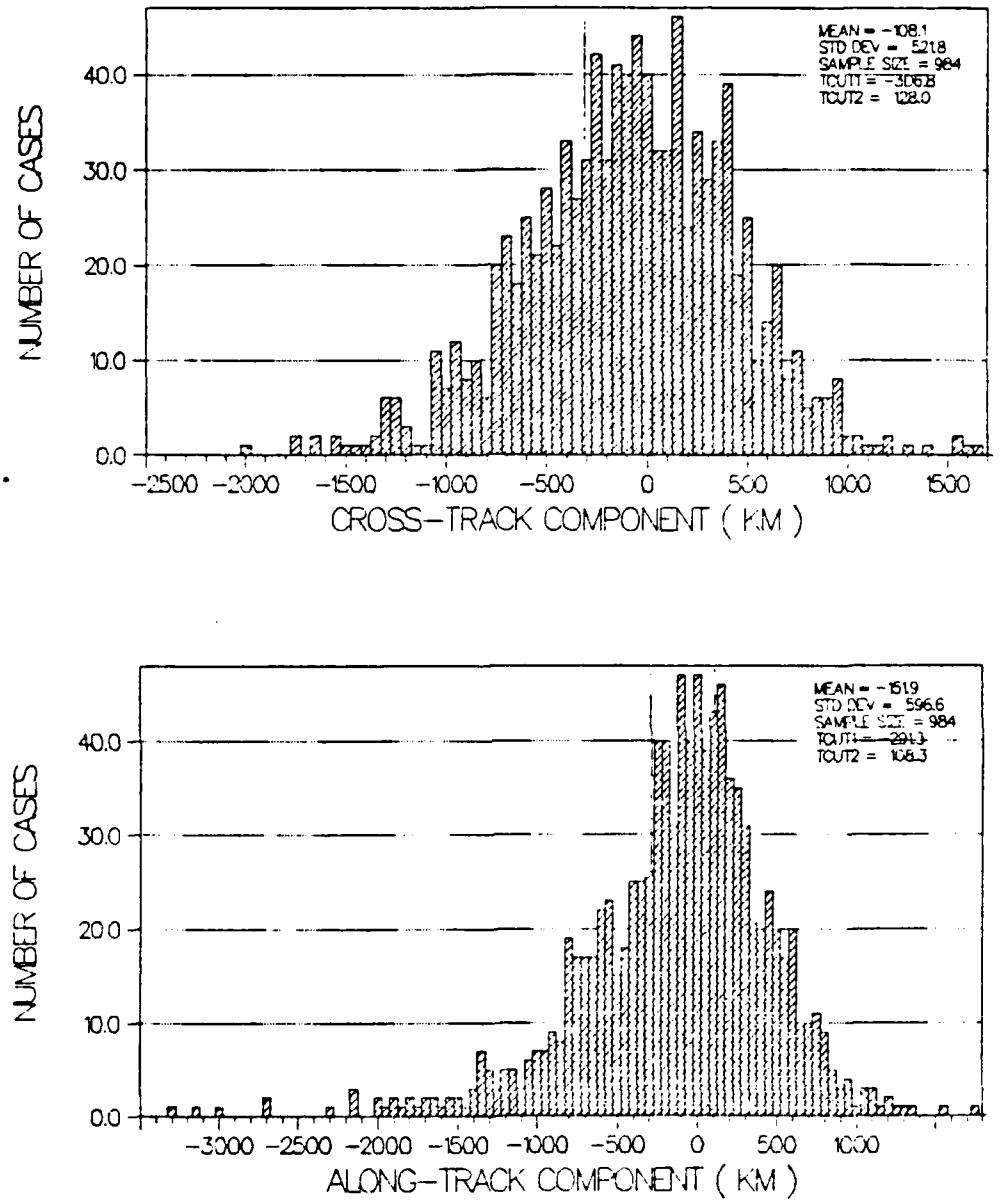

Fig. 4.1. Frequency distribution of the OTCM cross-track and along-track components (km) with respect to a CLIPER track.

D. CORRECTION VARIABLES FOR THE OTCM FORECASTS

Over the years, it has become apparent that dynamical models exhibit systematic errors in the forecast track relative to the actual tropical cyclone track (Elsberry and Frill, 1980). There are a number of causes for such errors. First, the models contain an incomplete representation of the physical processes in the tropical cyclone. Second, the poor resolution of the inner region of the cyclone can cause a systematic phase speed error due to numerical considerations. Third, the introduction of a bogus vortex can cause systematic directional errors. An overly intense vortex may result in excessive poleward components of motion. Finally, an important cause for systematic errors may be inadequate observations. When observations are absent, the wind analysis reverts toward the first-guess field. In the case of the OTCM, this could introduce a zonal wind bias since the meridional components due to transient features are absent in the first-guess field, 5% of which is the monthly climatology.

In the past, pre- and post-processing techniques have been used to minimize the systematic bias in a dynamical model. Shewchuk and Elsberry (1978) demonstrated a pre-processing technique for the OTCM. Adjustment of the initial wind fields are used to re-direct the predicted track toward a known direction of movement. A post-processing technique developed by Elsberry and Frill (1980) integrated the OTCM backward in time to compare with the known past positions of the cyclone. This backward integration of the model can be rather costly. Peak and Elsberry (1983) proposed a backward extrapolation as a cost-effective alternative. In this post-processing technique, the backward extrapolated positions are compared to warning positions. The basic premise is that errors that occur in the backward portion of the track may be used to help define the expected errors in the forward positions.

A goal of this study is to develop a post-processing method that adjusts the OTCM forecast positions to reduce the systematic errors of the model. The correction method is illustrated in Fig. 4.2. An OTCM forecast position is corrected by subtracting the post-processed cross-track (CTP) and along-track (ATP) components. A regression analysis will be used to develop equations to predict the required CTP and ATP adjustments to the OTCM forecast positions at 24, 48 and 72 h.

The CTP and ATP components are defined as

$$CTP = OCT - BCT \tag{4.1}$$

and

$$ATP = OAT - BAT, \tag{4.2}$$

where the best-track and CT/AT OTCM components are defined as BCT/BAT and OCT/OAT respectively. Thus, the CTP and ATP adjusts the OTCM position to the observed (best-track) position. A statistical summary of the CTP and ATP corrections is given in Table 11. A physical significance can be applied to the values found in this table. For example, a mean negative CTP implies the average forecast position for the OTCM is to the left of the verified position. A mean negative ATP for the early forecast times indicates the OTCM forecast is generally slow, although the OTCM is fast by 72 h (i.e., positive mean). At 72 h, the combination of a mean negative CTP (left) and a mean positive ATP (ahead) indicates that the OTCM may not be forecasting recurvature situations very well on the average.

The distributions of the desired CTP and ATP corrections at 72 h are illustrated in Fig. 4.3. Although the distributions are rather concentrated between -700 and 700

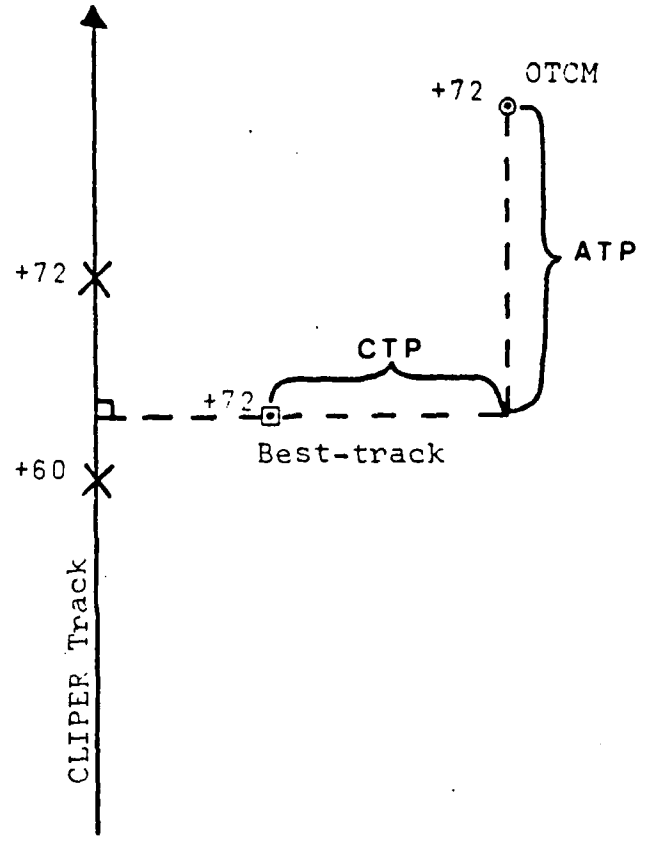

Fig. 4.2. Schematic of the OTCM modification scheme. Post-processed cross-track (CTP) and along-track (ATP) components adjust the OTCM forecast position to the best-track position.

Table 11. Mean ($\bar{X}$) and standard deviations (σ) of the post-processing components CTP and ATP (km) for OTCM forecasts during 1979-1983 (N = sample size).

		CTP		ATP	
Time	N	$\bar{X}$	σ	$\bar{X}$	σ
24	1083	18	172	-70	186
48	860	-35	324	-12	365
72	642	-118	508	103	509

km, there are a number of cases on the tails of the distribution where the OTCM errors (CTP and ATP) become very large. Hopefully, the errors in these cases should be improved in the statistical correction scheme to be developed.

E. REGRESSION ANALYSIS

Regression analysis is one of the most widely used statistical tools. Neter and Wasserman (1974) give an excellent presentation of the theory and method of regression analysis. Briefly, it involves using a linear combination of predictors to estimate the value of an unknown quantity, the predictand. A primary goal of the analysis is to choose a set of predictors that minimizes the sum of squares of residuals without overfitting.

1. Predictors

A set of predictors is sought to assess five factors affecting an OTCM forecast: (1) external (to the cyclone) physical forcing; (2) previous cyclone movement; (3) current cyclone intensity; (4) date; and (5) initial (warning) position. In addition, a set of post-processing predictors will be used to assess possible errors via a backward extrapolation of the track (Peak and Elsberry, 1983). A total of 187 possible predictors are generated (Table 12).

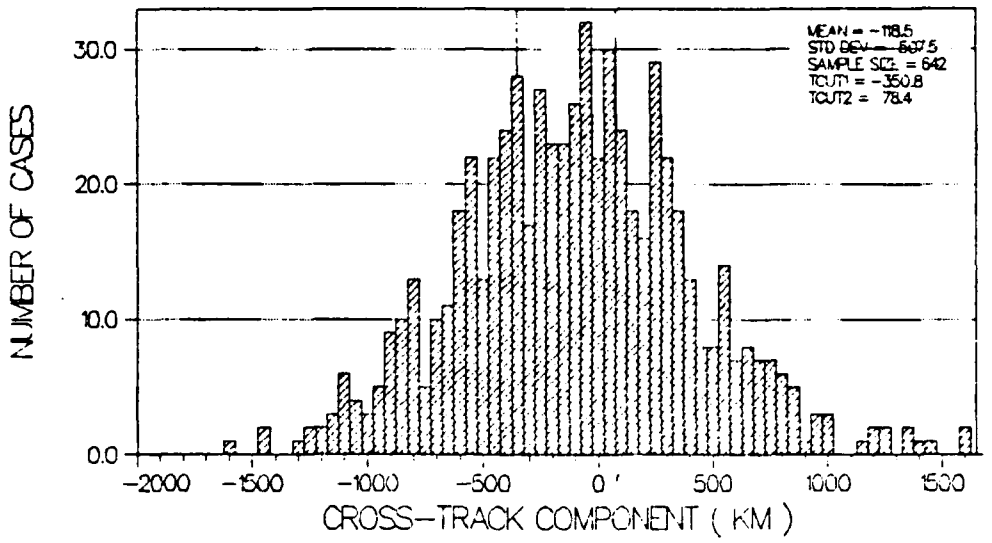

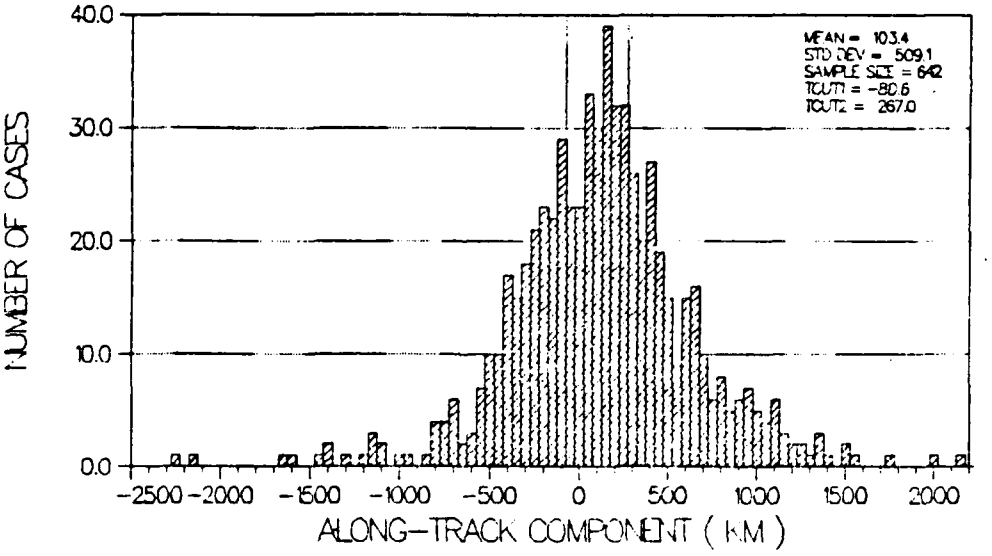

Fig. 4.3. Frequency distribution of the post-processed cross-track (CTP, top) and along-track (ATP, bottom) components (km). See definitions in (4.1) and (4.2).

Four potential predictors are related to the observations of the tropical cyclone at the base time. These include the Julian date, the JTWC warning latitude and longitude, and the maximum sustained wind speed (predictors 1 to 4 in Table 12).

The recent motion of the cyclone is an important predictor of most statistical forecast schemes. The OTCM forecasts are adjusted for a persistence component via the Shewchuk and Elsberry (1978) pre-processing scheme. However, nine potential predictors representing past motion are still included to evaluate OTCM's persistence component of motion (predictors 5 to 13 in Table 12). These past-motion predictors are based on JTWC warning positions to simulate operational conditions.

The EOF coefficients derived in Chapter 2 are used to represent quantitatively the environmental wind field. Wilson (1984) developed a promising regression track scheme using these EOF coefficients. In the present OTCM post-processing study, the predictor set includes only the first 25 zonal and meridional modes at each pressure level (predictors 14 to 163 in Table 12). Notice that the EOF coefficients are identified as Clwnn, where C identifies the predictor as a coefficient, l is the level (7 for 700, 4 for 400 and 2 for 250 mb), w is the wind component (u or v) and nn is the EOF mode number. It is anticipated that the synoptic wind forcing represented by the EOF coefficients will be key predictors in this regression scheme.

This study uses the backward extrapolation method of Peak and Elsberry (1983) to define a set of six additional predictors (Fig. 4.4). The +24 h OTCM position is extrapolated backwards to define a -24 h position. This position is compared to the -24 h warning position. The total, meridional and zonal distances (E24, EY24 and EX24) from the backward OTCM positions to the warning positions

Table 12. Potential predictors provided in the regression analysis.

Predictor Number	Name	Description
1	JULDATE	Julian date
2	LAT	Warning position latitude
3	LON	Warning position longitude
4	SPD	Maximum sustained wind speed (kts)
5	VX0012	Zonal cyclone movement from 00 to -12 h (km/hr)
6	VY0012	Meridional cyclone movement from 00 to -12 h (km/hr)
7	V0012	Total cyclone movement from 00 to -12 h (km)
8	VX1224	Zonal cyclone movement from -12 to -24 h (km/hr)
9	VY1224	Meridional cyclone movement from -12 to -24 h (km/hr)
10	V1224	Total cyclone movement from -12 to -24 h (km).
11	VX0024	Zonal cyclone movement from 00 to -24 m/hr).
12	VY0024	Meridional cyclone movement from 00 to -24 h (km/hr).
13	V0024	Total cyclone movement from 00 to -24 h (km).
14-38	C7U1-25	700 mb coefficients derived for zonal modes 1 to 25.
39-63	C7V1-25	700 mb coefficients derived for meridional modes 1 to 25.
64-88	C4U1-25	400 mb coefficients derived for zonal modes 1 to 25.
89-113	C4V1-25	400 mb coefficients derived for meridional modes 1 to 25.
114-138	C2U1-25	250 mb coefficients derived for zonal modes 1 to 25.
139-163	C2V1-25	250 mb coefficients derived for meridional modes 1 to 25.
164-166	E12, EY12, EX12	Dist. from 12 h backward extrapolation pt. to -12 h warning position. Meridional and zonal dist. included.
167-169	E24, EY24, EX24	Dist. from 24 h backward extrapolation pt. to -24 h warning position. Meridional and zonal dist. included.
170-172	D2400, DY2400, DX2400	Dist. from 24 h OTCM position to 00 h warning position. Meridional and zonal dist. included.
173-175	D4800, DY4800, DX4800	Dist. from 48 h OTCM position to 00 h warning position. Meridional and zonal dist. included.
176-178	D4824, DY4824, DX4824	Dist. from 48 h OTCM position to 24 h OTCM position. Meridional and zonal dist. included.
179-181	D7200, DY7200, DX7200	Dist. from 72 h OTCM position to 00 h warning position. Meridional and zonal dist. included.
181-184	D7248, DY7224, DX7224	Dist. from 72 h OTCM position to 48 h OTCM position. Meridional and zonal dist. included.
184-187	D7224, DY7224, DX7224	Dist. from 72 h OTCM position to 24 h OTCM position. Meridional and zonal dist. included.

are used as potential predictors. The same procedure is used to define E12, EX12 and EY12. However, since the 12 h OTCM position is not available, the backward 12 h OTCM position is calculated by taking one half of the distance of the 24 h position, and projecting this value backward.

An additional set of predictors (170 to 187 in Table 12) is used to characterize the forward portion of the OTCM forecast track (Fig. 4.4). It is hypothesized that these forward track predictors may explain a portion of the variance in CTP and ATP by distinguishing beteen different forecast track orientations. For example, the magnitude of the zonal track distance between 72 and 24 h (DX7224) may explain some of the variance in CTP at 72 due to recurving storms.

2. Dependent Sample

It is very important that the regression scheme simulate operational conditions. An OTCM forecast to provide guidance at 00 and 12 GMT must be initiated from the 12-h old prediction fields (Fig. 4.5) because the rawinsonde reports are not received at FNOC until several hours past the synoptic times. An OTCM prediction at 06 and 18 GMT (actually integrated at about 0730 and 1930) is initiated with the 00 and 12 GMT analysis fields. This situation is chosen to develop a dependent sample for the regression analysis. That is, the GBA wind fields from 00 and 12 GMT are matched with the 06 and 18 GMT OTCM predictions. The development of a dependent sample in this way ensures that the regression analysis scheme will be consistent with the current operational version of the OTCM. The 00 and 12 GMT OTCM forecasts can not be used because the 12-h predicted wind fields are not available for this study. Unfortunately, the OTCM was either not requested at 06 and 18 GMT or the forecasts were not archived from 1979-1981, because only four 06 and 18 GMT OTCM forecasts are available

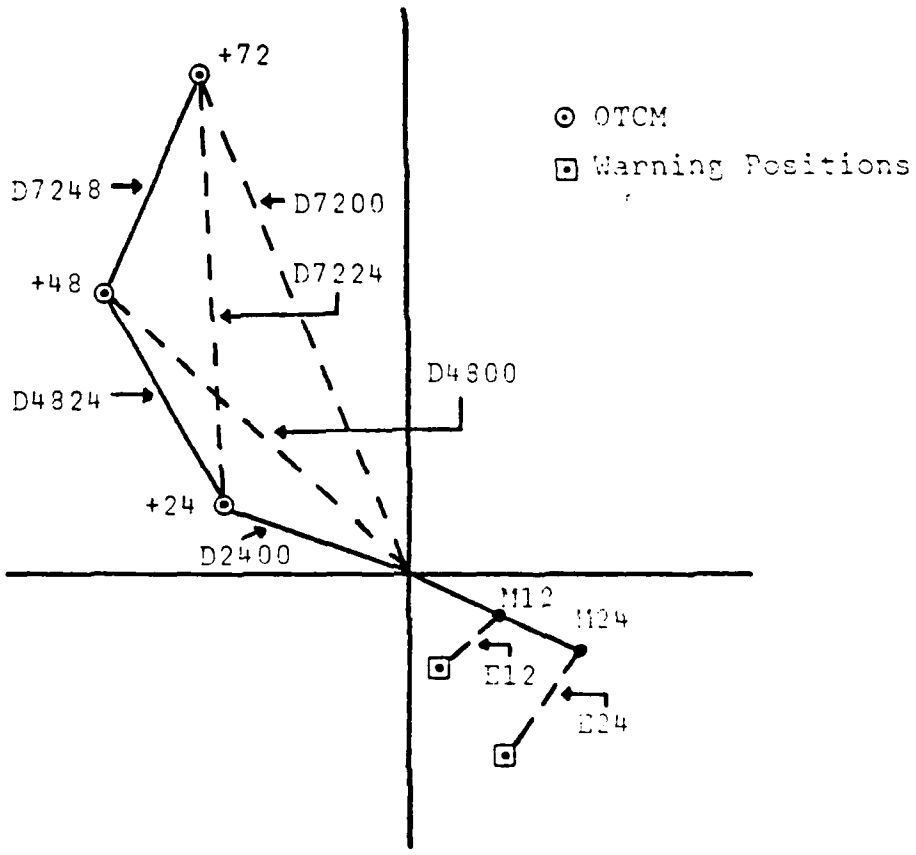

Fig. 4.4. Schematic illustration of OTCM forecast positions (+24, +48, +72) and backward extrapolation positions (M12 and M24). Other identifiers are defined in Table 12. The displacements identified by dashed lines, along with the corresponding zonal and meridional component displacements (not shown), are used as potential predictors in the regression analysis.

from 1979-1981. Therefore, the dependent sample consists almost entirely of OTCM forecasts from 1982-1983. After the OTCM forecasts are matched with the wind-based EOF cases, the sample size was reduced to 161 cases at 72 h. Since the sample size is small, withholding cases for an independent sample is not possible.

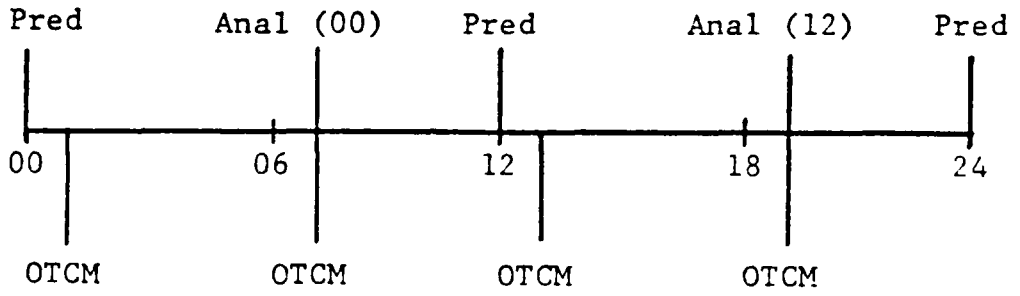

Fig. 4.5. Schematic showing execution times for the One-way Tropical Cyclone Model during a 24-h period. The initial fields for the dynamical model are either 12 h prediction fields or the 7 h old analysis fields.

3. Prediction Equations

A linear stepwise regression analysis is chosen to predict the CTP and ATP adjustments to the OTCM forecast positions. The UCLA Biomedical computer program BMDP2R (Dixon and Brown, 1979) is used for the analysis. The stepwise regression analysis ensures that a potential predictor is not included in the equation if it is highly correlated with any predictor chosen in earlier steps. A minimum F-to-enter value of 4.0 is imposed to ensure that the predictor is significantly correlated with the predictand (Dixon and Brown, 1979).

Two separate regression schemes are developed. The first scheme uses only the EOF coefficients as potential

Table 13. Explained variance (R^2) for the CTP and ATP for regression scheme COE in which only EOF coefficients are included as predictors and ALL in which all potential predictors are permitted. Separate entries are given for sets limited to a maximum of 5 or 10 predictors (* indicates only nine predictors selected).

Time	N	Number of Predictors	Regression Scheme	R^2 CTP	R^2 ATP
24	267	5	COE	0.24	0.19
		10	COE	0.34	0.29
		5	ALL	0.33	0.33
		10	ALL	0.44	0.44
48	212	5	COE	0.27	0.27
		10	COE	0.36	0.40
		5	ALL	0.37	0.35
		10	ALL	*0.44	0.47
72	161	5	COE	0.35	0.29
		10	COE	0.48	0.44
		5	ALL	0.42	0.33
		10	ALL	0.55	0.53

predictors (referred to as COE in later tables). It was demonstrated in Chapter 3 that the wind-based EOF coefficients can be used to represent synoptic forcing of tropical cyclone motion. It is hypothesized that these coefficients will also explain a significant portion of the variance in the CTP and ATP components. The second set of regression equations uses all of the potential predictors found in Table 12 (referred to as ALL in later tables). Comparison of the predictors selected in the two sets and the additional skill produced by the ALL set will indicate the relative importance of the EOF coefficients.

The amount of variance explained by the predictors is indicated by the R^2, which is defined as

$$R^2 = SSR/SSTO = 1 - (SSE/SSTO), \qquad (4.3)$$

where SSTO is the total sum of squares, SSR is the regression sum of squares and SSE is the residual sum of squares. An R^2 value of 1.00 would indicate that the regression equation explains all the variance in the

predictand (i.e., CTP or ATP). The R^2 values for both the CTP and ATP regression sets are summarized in Table 13. The amount of variance explained by the equations ranges from 19% to 55%. As expected, the regression set that uses all of the potential predictors explains the largest amount of variance (Table 13). For example, 55% of the variance in CTP at 72 h is explained by ten predictors in the ALL scheme. It is extremely encouraging that the largest amount of variance is explained by the regression equations at the 72-h forecast interval.

The regression equation for CTP at 72 h (CTP72) is shown in Table 14. The CTP72 ajustment is obtained by summing the product of the regression coefficients (column 2) and the values of the associated predictors. The first predictor explains 18% of the variance in CTP72 (i.e., R^2 = 0.18). The second predictor explains an additional 11%, and so on. Although 3% of the variance in CTP72 is explained by the 10th predictor, the equation is arbitrarily limited to this number of variables. Addition of a large number of variables may artificially inflate the explained variance and yet produce unstable equations when used with an independent sample.

The regression equations for CTP and ATP developed using all potential predictors are shown in Tables 15 and 16 respectively. Corresponding regression equations for the coefficients-only (COE) scheme are found in the Appendix, Tables 20 and 21. Notice that the EY12 predictor is selected early at all three forecast intervals in Table 15. The backward extrapolation variable EY12 is a measure of how closely the initial forecast track of the OTCM agrees with a meridional component of motion based on persistence. That is, future errors in the OTCM forecast track are highly correlated with the departure of the OTCM from a persistence component of motion early in the forecast period.

Table 14. Regression equation for CTP (km) at 72 h using all potential predictors (see Table 12) in the regression analysis. R^2 is the amount of variance explained by the predictor. Mean ($\bar{x}$) and standard deviation (σ) for the predictors are included.

Intercept -11.8

Predictor	Coefficient	R^2	$\bar{X}$	σ
C7U7	48.4	0.18	-0.5	4.0
C2V1	24.7	0.11	1.1	4.8
EY12	1.3	0.06	33.0	105
C4V3	-26.0	0.04	-1.3	4.5
C4U20	-77.6	0.03	-0.2	1.7
C7U21	46.7	0.03	0.4	1.9
C2V21	46.2	0.02	0.2	2.2
C7U2	17.0	0.02	3.3	7.5
C7V16	-30.7	0.03	0.1	2.7
D7224	-0.3	0.03	839	298
	Total	0.55		

The most frequently chosen predictors are the wind-based EOF coefficients (Table 17). In the ALL scheme, the EOF coefficients comprise between six and eight of the ten predictors picked in the regression analysis. The u coefficients at 700 mb are most often picked (15 times), while the u coefficients at 250 mb are the least often picked (one time). It is interesting that the 400 mb u coefficients are selected to correct the relative speed (ATP) of the OTCM, whereas the 700 mb u coefficients are selected most frequently to adjust the directional (CTP) aspect of the track.

Several potential predictors are not included in any of the equations. The only purely persistence predictor selected is the -12 to -24 meridional motion (VY1224) in the CTP24 regression equation. This does not necessarily indicate that the pre-processing aspect of the OTCM accounts perfectly for departures from a persistence track. The early selection of EY12 predictor, which is also related to a departure from persistence, probably explains why the other persistence-related predictors are not selected.

Table 15. Regression equations for CTP (km) at the 24, 48 and 72 h forecast intervals (the ALL scheme). The order in which the predictors are selected in the equations is indicated within the parentheses.

	Forecast Interval (h) 24	48	72
Intercept	-3.766	-60.312	-11.844
Predictor			
C7U7	6.713 (8)	29.602 (2)	48.398 (1)
C2V1	-	13.107 (3)	24.715 (2)
EY12	0.332 (1)	0.754 (1)	1.262 (3)
C4V3	-	-	-26.023 (4)
C4U20	-	-	-77.641 (5)
C7U21	-	32.112 (5)	46.682 (6)
C2V21	-	-	46.211 (7)
C7U2	-	-	17.049 (8)
C7V16	-	-	-30.744 (9)
D7224	-	-	-0.286 (10)
C7V9	7.400 (5)	12.021 (4)	-
C7V23	-	20.412 (6)	-
C4U13	-	-18.895 (7)	-
C4V19	-	14.063 (8)	-
C4V10	-	11.032 (9)	-
EX24	0.332 (2)	-	-
C4U6	-12.095 (3)	-	-
C7U9	8.449 (4)	-	-
C4V2	4.632 (6)	-	-
C7U17	-9.539 (7)	-	-
C4V11	6.393 (9)	-	-
C7U16	9.086 (10)	-	-

4. Verification

The potential performance of these regression equations is tested on the dependent sample. The regression-predicted CTP and ATP components are used to modify the OTCM position (referred to as OTCMP in later tables). The forecast error is computed by determining the great circle distance from the modified OTCM position to the best-track position. The forecast errors for the modified and unmodified OTCM forecasts are summarized in Tables 18 and 19. The official (JTWC) forecast errors for the corresponding cases (when available) are also included in the tables. The (unmodified) OTCM forecast errors are smaller than the official JTWC forecasts (Tables 18 and 19).

Table 16. As in Table 15, except for regression equations for ATP (km).

	Forecast Interval (h) 24	48	72
Intercept	184.124	141.880	292.125
Predictor			
C7U14	-	-	49.924 (1)
C4U5	-	-	16.565 (2)
C4V24	-	-	34.195 (3)
DX7248	-	-	1.344 (4)
C7V7	-	-	31.895 (5)
C7U12	-	-33.034 (5)	-53.297 (6)
EY12	-	-1.423 (2)	-1.350 (7)
XLAT	-12.802 (2)	-15.218 (8)	-31.400 (8)
C2U23	-	-	-59.994 (9)
C4U12	-8.819 (8)	-39.319 (1)	-30.182 (10)
C4U15	-	-21.200 (3)	-
C7U24	-	30.980 (4)	-
DX7224	-	0.292 (6)	-
C4U16	-10.949 (5)	-25.067 (7)	-
C2V24	13.105 (7)	24.426 (9)	-
C7U10	-	-12.878 (10)	-
E12	-0.545 (1)	-	-
C2U5	-6.673 (3)	-	-
C7U7	-11.055 (4)	-	-
VY1224	4.933 (6)	-	-
C4U10	10.836 (9)	-	-
C4V15	-8.008 (10)	-	-

Table 17. The number of EOF coefficients selected in the regression scheme ALL for the 24, 48 and 72 h equations for CTP and ATP.

Level	Field	CTP 24	CTP 48	CTP 72	ATP 24	ATP 48	ATP 72	Total
700	u	4	2	3	1	3	2	15
	v	1	2	1	0	0	1	5
400	u	1	1	1	3	3	2	11
	v	2	2	1	1	0	1	7
250	u	0	0	0	0	0	1	1
	v	0	0	2	1	1	0	4
Total		8	7	8	6	7	7	43

As expected, the mean forecast error increases as the forecast interval increases. Notice that the mean and standard deviations of the forecast errors at all times are smaller for the regression schemes (OTCMP) with either five or ten predictors than for the unmodified OTCM. A small improvement is found in the means and standard deviations when ten versus five predictors are used in the regression equations. As expected, the errors for the EOF coefficient only-scheme (Table 18) are larger than the errors for the other regression scheme, which includes all the predictors (Table 19). It is very encouraging that the regression schemes developed to modify the OTCM have reduced the mean forecast error at 72 h by over 210 km (Table 19). It is again emphasized that these results are obtained using the dependent sample. Independent testing is required to determine if the equations are stable.

Table 18. Mean ($\bar{X}$) and standard deviation (σ) of the forecast errors (km) for the regression scheme which uses EOF coefficients only (OTCMP) with either 5 or 10 predictors. Also included are forecast errors for a homogeneous set of unmodified OTCM forecasts and a nearly homogeneous set of JTWC forecasts.

Time	N	Number of Predictors	Method	Forecast Errors $\bar{X}$	σ
24	245	-	JTWC	206	127
	"	-	OTCM	203	121
	"	5	OTCMP	162	102
	"	10	OTCMP	158	95
48	190	-	JTWC	443	285
	200	-	OTCM	386	202
	"	5	OTCMP	329	192
	"	10	OTCMP	311	163
72	151	-	JTWC	631	400
	161	-	OTCM	593	357
	"	5	OTCMP	484	313
	"	10	OTCMP	427	279

A desirable feature in any forecast scheme is consistency, which is indicated by small standard deviations

Table 19. As in Table 18, except for regression scheme which uses all potential predictors (OTCMP) with either 5 or 10 predictors.

Time	N	Number of Predictors	Method	Forecast Errors $\bar{X}$	σ
24	245	-	JTWC	206	127
	"	-	OTCM	203	121
	"	5	OTCMP	157	95
	"	10	OTCMP	143	88
48	190	-	JTWC	443	285
	200	-	OTCM	386	202
	"	5	OTCMP	302	177
	"	10	OTCMP	286	148
72	151	-	JTWC	631	400
	161	-	OTCM	593	357
	"	5	OTCMP	452	286
	"	10	OTCMP	383	256

in the forecast errors. Thus, it is significant that the standard deviations for the ALL regression scheme are about 100 km smaller than those of the unmodified OTCM (Table 19). This result, along with lower mean forecast errors, indicates the regression equations are extremely successful in modifying the OTCM in this dependent sample.

A schematic representation of the performance of the regression scheme using all potential predictors is illustrated in Fig. 4.6. A perfect regression scheme would have resulted in all of the cases lying on the y=x line. The correlation coefficient between the observed and predicted CTP values is 0.74. The correlation coefficient for the ATP distribution is 0.73. When there are large errors in the observed CTP and ATP, the regression scheme can be very successful in adjusting the OTCM to correct for those errors. However, there are also times when the modification actually degrades the OTCM forecast.

In summary, two regression schemes are developed. The first set uses only the wind-based EOF coefficients as potential predictors and the second set uses all the

potential predictors in Table 12. The EOF coefficients are frequently selected, although the backward extrapolation variable EY12 is often the first predictor selected at all forecast intervals. This suggests a high correlation exists between the OTCM's departure from persistence and future track errors. Testing of the regression equations on the dependent sample shows the scheme to be very successful in reducing the mean forecast errors and the standard deviations. The reduction in the standard deviation indicates that the modified OTCM forecasts are more consistent than the unmodified ones. Independent sample testing is not possible since all available cases have been used to develop the regression equations.

F. CAUTIONS FOR THE USE OF THE REGRESSION MODEL

The performance of the regression model on the dependent sample is likely to be superior to that from a new sample of cases. Such a prediction bias may occur if the predictors for the regression model are uniquely related to the dependent data cases. The performance of the regression model with independent cases depends upon whether conditions for the independent case are similar to those used to develop the regression model.

The forecaster should be aware of when to use or not use the regression scheme. For example, the forecaster should examine rare event situations, such as multiple cyclones, as the regression scheme may not perform very well for such events.

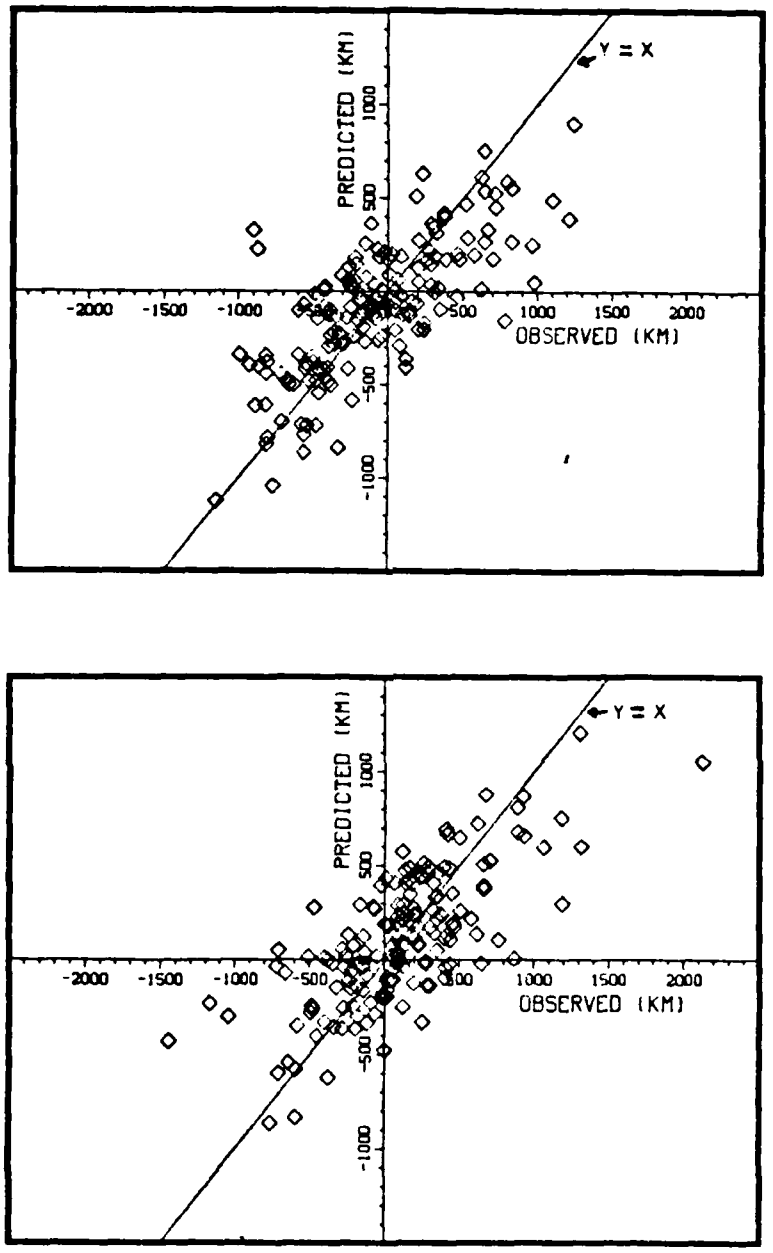

Fig. 4.6. Scatter plots of predicted versus observed CTP (top) and ATP (bottom) components. The predictions are from the 10-predictor regression scheme using all potential predictors.

V. CONCLUSIONS AND SUGGESTED RESEARCH

Using an EOF representation of the wind fields around a tropical cyclone, Wilson (1984) developed a successful statistical track prediction scheme. This study has further demonstrated that these EOF coefficients can be used to describe synoptic effects on tropical cyclone motion. Composite zonal and meridional wind fields have been calculated for five tropical cyclone categories defined in terms of the past 12-h motion of the cyclone. Different synoptic flow patterns are found in the environments of vortices that were moving northwestward (Category 4) and those moving northeastward (Category 5). Statistically significant differences in the u or v components based on a Student's t-test are found between wind fields in Category 4 and those in the other four categories. The number of significant points over the horizontal grid ranged from 96 to 491 out of a possible 527 points. The results of these t-tests (Table 7) provide statistical support for the hypothesis that the wind fields for Category 4 storms are different from those for storms in the other four categories.

Sets of regression equations are also developed to post-process the One-way Tropical Cyclone Model (OTCM). Although the backward-extrapolated predictors introduced by Peak and Elsberry (1983) are often selected first, the wind-based EOF coefficients are frequently selected. The schemes are extremely successful in reducing forecast errors based on tests with the dependent sample. For example, the mean OTCM forecast error at 72 h is 593 km, whereas the mean error for the best regression scheme is only 383 km. The regression schemes also reduces the standard deviations of the forecast errors by as much as 100 km. This reduction

indicates that the regression-modified OTCM forecasts are more consistent than the unmodified OTCM. Therefore, it appears that the regression scheme has great potential for operational applications.

A. POTENTIAL FOR USE WITH INDEPENDENT DATA

It has been demonstrated that the EOF coefficients provide a large portion of the error reduction in the OTCM track positions. These EOF coefficients are synoptic predictors in that they represent the flow fields surrounding the tropical cyclone. For a new case, the EOF coefficients would be derived using the eigenvectors from the dependent sample cases. It is stressed that about half of the wind-based EOF coefficients in this study have been derived using Wilson's dependent eigenvector matrix. Wilson (1984) demonstrated that the eigenvectors derived from the dependent sample should be stable since the dependent sample size is large (682 cases). However, testing is required to determine that the present sample size is sufficient to ensure stability. The reader is referred to Shaffer (1982) for a detailed example of the appropriate methodology to test for stability.

The regression schemes developed in this study have not been tested with independent data. New predictors associated with an independent case may differ significantly from the dependent sample predictors. When this occurs, the performance characteristics of the model are likely to be degraded. Therefore, testing on independent data is required before the regression scheme can be implemented operationally.

B. OPERATIONAL IMPLEMENTATION

The regression model developed in this study applies only to the 06 and 18 GMT OTCM predictions. No regression model is developed for the 00 and and 12 GMT OTCM forecasts,

which are initialized using 12-h old analysis fields that have been slightly adjusted towards climatology in the tropics. These adjusted wind fields are not available for deriving the EOF coefficients required in this study.

There are operational limitations for the regression scheme developed in this study. The 00 and 12 GMT GBA must be available for the EOF analysis. The same storm selection criteria described in Chapter 2 has to be used in an operational version. Finally, the tropical cyclone must satisfy the conditions necessary for making a CLIPER forecast (see Chapter 2, section C).

The operational implementation of the regression scheme would be straight-forward. Four operations are required for implementation. First, the 25 required EOF coefficients must be calculated for each new case. The GBA zonal and meridional wind components at 700, 400 and 250 mb must be interpolated onto the equidistant grid using the bilinear interpolation method (Wilson, 1984). The EOF coefficients would then be derived by multiplying the transpose of the truncated eigenvector matrix (25 X 527) and the normalized observational matrix (527 X 1) for the new case. No significant error is anticipated from normalization using the means and standard deviations from Wilson's dependent sample. The second step for implementation would be to activate the OTCM and CLIPER models, and calculate the OTCM cross-track and along-track components with respect to the CLIPER track. The third step would be to calculate the remaining predictors included in the regression equations. Finally, the appropriate predictors would be substituted into the set of regression equations to predict the OTCM modification values CTP and ATP at 24, 48 and 72 h. Both the modified and unmodified tracks would then be transmitted to JTWC. As all the information necessary to apply the regression modification to the OTCM is available at FNOC,

less than one minute of additional computer time would be required to also provide the modified OTCM track to JTWC.

C. SUGGESTED RESEARCH

Although the regression scheme developed in this study produces very good results, it may be further improved if other storm-related or synoptic predictors are provided for the regression analysis. For example, the size of the tropical cyclone (as defined by the radius of 30 kt winds) could be used. Another example would be to use EOF coefficients derived from predicted wind fields, such as the 24-h forecast from the global prediction model. These EOF coefficient predictors might have great potential for improving the regression scheme at longer forecast intervals. If the wind fields used to initialize the 00 and 12 GMT OTCM forecasts were archived, a similar procedure as in this study could be used to develop regression equations for modifying these OTCM tracks.

Since the post-processing procedure proposed in this study has shown great potential in reducing forecast errors from the OTCM, the same technique could be used to modify other forecast aids provided to JTWC. For example, a modified Nested Tropical Cyclone Model track could be easily implemented using the procedure described in Chapter 4.

The decision-tree approach introduced by Peak and Elsberry (1985) could also be tested as an adjustment technique for the OTCM. The algorithm developed by Breiman et al. (1984) provides a decision tree with multiple branches. Each branch represents a sub-division of the data based on the best available predictor for splitting. The result is a tree which classifies similar cases and provides key values of the classification. The least accurate branches are pruned by repeatedly determining the minimum errors in the prediction using subsets of the test sample. Each branch ultimately ends in a terminal node. A

statistical summary of the number of successful and unsuccessful classifications in that node from the dependent sample provides a measure of the likely accuracy of the classification. The probability measure for each terminal node would suggest the confidence that the forecaster should have in that guidance. It seems likely that the wind-based EOF coefficients would provide useful predictors for developing such a decision tree.

In Wilson (1984) and the present study, the wind field is decomposed into zonal and meridional components to do a scalar EOF analysis. However, a vector EOF analysis of the total winds (Legler, 1983) also may be developed to determine the possibility of improving the regression forecast scheme. In addition, it would be useful to examine the effect of rotation of the eigenvectors as suggested by Richman (1981).

In conclusion, the wind-based EOF coefficients provide an efficient and accurate representation of the synoptic wind forcing of tropical cyclone motion. Given this scientific basis, application to regression schemes to improve tropical cyclone forecasts seems feasible. Further research with the wind-based EOF fields is warranted.

APPENDIX

Table 20. Regression equations for CTP (km) at the 24, 48 and 72 h forecast intervals (the COF scheme). The order in which the variables are selected in the equations is indicated within the parentheses.

	Forecast Interval (h)		
	24	48	72
Intercept	6.7	-23.2	292.1
Predictor			
C7U7	8.8 (2)	31.2 (1)	49.7 (1)
C2V1	-	13.8 (2)	41.7 (2)
C7U6	-	-	43.4 (3)
C7V3	-	-	-37.2 (4)
C2V21	-	-	43.5 (5)
C7U13	-	-	-38.7 (6)
C7V20	-	-	48.5 (7)
C2V9	-	-	-27.7 (8)
C7U10	-	-	26.8 (9)
C4U12	-	-	-32.8 (10)
C7V9	-	11.5 (3)	-
C2V17	-	21.3 (4)	-
C2U14	-	-33.4 (5)	-
C2U15	-	-26.2 (6)	-
C2U6	-	13.4 (7)	-
C4U13	-	-24.4 (8)	-
C4V23	-	19.8 (9)	-
C7V23	-	18.4 (10)	-
C2U1	5.5 (1)	-	-
C4U15	-15.4 (3)	-	-
C7U21	15.0 (4)	-	-
C7U25	-18.9 (5)	-	-
C2V16	10.9 (6)	-	-
C2U12	-11.9 (7)	-	-
C2V3	-5.6 (8)	-	-
C2U4	7.9 (9)	-	-
C7U4	4.2 (10)	-	-

Table 21. As in Table 20, except for regression equations for ATP (km).

	Forecast Interval (h)		
	24	48	72
Intercept	-69.0	-37.3	-5.9
Predictor			
C4U12	-13.6 (6)	-52.8 (1)	-52.1 (1)
C4V14	-	-25.0 (3)	-34.8 (2)
C2V13	-	-25.8 (6)	-38.1 (3)
C7V7	-	-	14.5 (4)
C4V24	-	-	66.1 (5)
C2V20	-	-	-44.1 (6)
C4U5	-	15.0 (8)	29.2 (7)
C7U16	-	-	45.9 (8)
C7U14	-	-	34.6 (9)
C2V6	-9.0 (5)	-17.0 (5)	-15.3 (10)
C7U24	-	35.5 (2)	-
C2V24	9.1 (10)	25.7 (4)	-
C4U24	-	-42.8 (7)	-
C7U7	-13.0 (3)	-14.9 (9)	-
C7V24	-	-22.5 (10)	-
C2U5	-5.0 (1)	-	-
C7V3	-4.4 (2)	-	-
C4V18	-9.6 (4)	-	-
C7U25	-18.9 (5)	-	-
C4V5	9.1 (7)	-	-
C4V20	-12.1 (8)	-	-
C7U19	8.7 (9)	-	-

LIST OF REFERENCES

Breiman, L., J. H. Friedman, R. A. Olshen, and C. J. Stone, 1984: Classification and Regression Trees, Wadsworth Inc., 358 pp.

Brown, D. W., 1981: Tropical storm movement forecasting based on synoptic map typing using Empirical Orthogonal Functions. M. S. Thesis, Naval Postgraduate School, Monterey, CA, 80pp.

Chan, J. C.-L., 1985: Identification of the steering flow for tropical cyclone motion from objectively analyzed wind fields. Mon. Wea. Rev., 113, 106-116.

Dixon, W. J., and M. B. Brown, 1979: BMDP Biomedical Computer Program P-Series, University of California Press, Berkley California, pp. 367-460.

Elsberry, R. L., and D. R. Frill, 1980: Statistical post-processing of dynamical tropical cyclone model track forecasts. Mon. Wea. Rev., 108, 1219-1225.

Elsberry, R. L., and J. E. Peak, 1986: An evaluation of tropical forecast aids based on cross-track and along-track components. Mon. Wea. Rev., (in press).

Fiorino, M., 1985: Operational numerical modeling of tropical cyclone motion. WMO International Workshop on Tropical Cyclones, Bangkok, Thailand, in press.

Hardy, D. M., and J. J. Walton, 1978: Principal component analysis of vector wind measurements. J. Appl. Meteor., 17, 1153-1162.

Harrison, E. J., Jr., 1981: Initial results from the Navy two-way interactive nested tropical cyclone model. Mon. Wea. Rev., 109, 173-177.

Hodur, R. M., and S. D. Burk, 1978: The Fleet Numerical Weather Central Tropical Cyclone Model: Comparison of cyclic and one-way interactive boundary conditions. Mon. Wea. Rev., 106, 1665-1671.

Jarrell, J. D., and W. L. Somervell, Jr., 1970: A computer technique for using typhoon analogues as a forecast aid. NAVWEARSCHFAC Tech. Pap. 6-70, 47 pp (NTIS AD A008860).

Jarrell, J. D., S. Brand and D. S. Nicklin, 1978: An analysis of western North Pacific tropical cyclone forecast errors. Mon. Wea. Rev., 106, 925-937.

Kutzbach, J. E., 1967: Empirical eigenvectors of sea-level pressure, surface temperature and precipitation complexes over North America. J. Appl. Meteor., 6, 791-802.

Legler, D. M., 1983: Empirical orthogonal function analysis of wind vectors over the tropical Pacific region. Bull. Amer. Meteor. Soc., 64, 234-241.

AD-A164 170 APPLICATIONS OF WIND EMPIRICAL ORTHOGONAL FUNCTIONS IN TROPICAL CYCLONE MOTION STUDIES(U) NAVAL POSTGRADUATE SCHOOL MONTEREY CA T B SCHOTT DEC 85 2/2

UNCLASSIFIED F/G 4/2 NL

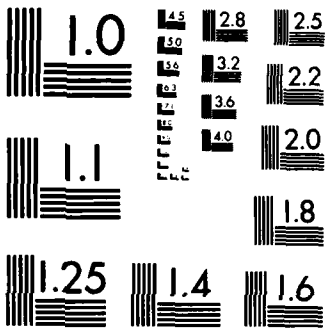

Lorenz, E. N., 1956: Empirical orthogonal functions and statistical weather predictions. Department of Meteorology, Massachusetts Institute of Technology, Cambridge, Massachusetts. Scentific Report 1, Statistical Forecasting Project, 48 pp.

Morrison, D. F., 1967: Multivariate Statistical Methods. McGraw-Hill (ed. 2, 1976), 338 pp.

Neter, J., and W. Wasserman, 1974: Applied Linear Statistical Models. Richard D. Irwin, Inc., Romewood, IL, 842 pp.

Neumann, C. J., and M. B. Lawrence, 1975: An operational experiment in the statistical-dynamical prediction of tropical cyclone motion. Mon. Wea. Rev., 103, 665-673.

Neumann, C. J., and J. M. Pelissier, 1981: Models for the prediction of tropical cyclone motion over the North Atlantic: an operational evaluation. Mon. Wea. Rev., 109, 522-538.

Peak, J. E., and R. L. Elsberry, 1983: A simplified statistical post-processing technique for adjusting tropical cyclone tracks. Pap. Meteor. Res., No. 5, 1-14.

Peak, J. E., and R. L. Elsberry, 1985: Objective selection of optimum tropical cyclone guidance using a decision-tree methodology. Extended abstracts, 16th Tech. Conf. on Hurricanes and Tropical Meteorology, Houston, Amer. Meteor. Soc.,97-98.

Peak, J. E., and R. L. Elsberry, 1986: Prediction of tropical cyclone turning and acceleration using empirical orthogonal function representations. Mon. Wea. Rev., (in press).

Preisendorfer, R. W., and T. P. Barnett, 1977: Significance tests for empirical orthogonal functions. Proceedings from the 5th Conference on Probability and Statistics in Meteorology and Atmospheric Science, Amer. Meteor. Soc., Boston, MA, 169-172.

Richman, M. B., 1981: Obliquely rotated principal components: an improved map typing technique? J. Appl. Meteor., 20, 1145-1159.

Riehl, H., W. H. Haggard and R. W. Sanborn, 1956: On the prediction of 24-hour hurricane motion. J. Meteor., 13, 415-420.

Sanders, F., and R. W. Burpee, 1968: Experiments in barotropic hurricane track forecasting. J. Appl. Meteor., 7, 313-323.

Sandgathe, S. A., 1985: Operational considerations for the Design of an Advance Tropical Cyclone Model. Appendix C, Naval Environmental Prediction Research Facility, Tech. Rep. TR 85-03, 152 pp.

Shaffer, A. R., 1982: Typhoon motion forecasting using empirical orthogonal function analysis of the synoptic forcing. M. S. Thesis, Naval Postgraduate School, Monterey, CA, 150 pp.

Shaffer, A. R., and R. L. Elsberry, 1982: A statistical climatological tropical cyclone track prediction technique using an EOF representation of the synoptic forcing. Mon. Wea. Rev., 110, 1945-1954.

Shapiro, L. J., and C. J. Neumann, 1984: On the structure and orientation of grid systems for the statistical prediction of tropical cyclone motion. Mon. Wea. Rev., 112, 188-199.

Shewchuk, J. D., and R. L. Elsberry, 1978: Improvement of short-term dynamical tropical cyclone motion prediction by initial field adjustments. Mon. Wea. Rev., 106, 713-718.

Stidd, C. K., 1967: The use of eigenvectors for climatic estimation. J. Appl. Meteor., 6, 255-264.

Tsui, T. L., 1984: A selection technique for tropical cyclone objective forecast aids. Postprints, 15th Conf. on Hurricanes and Tropical Meteorology, Amer. Meteor. Soc., Boston, 40-44.

U. S. Naval Weather Service, 1975: Numerical Environmental Products Manual. NAVAIR 50-1G-522, 155 pp.

Wilson, W. E., 1984: Forecasting of tropical cyclone motion using an EOF representation of wind forcing. M. S. Thesis, Naval Postgraduate School, Monterey, CA, 86pp.

Xu, Y., and C. J. Neumann, 1985: A statistical model for the prediction of western North Pacific tropical cyclone motion (WPCLPR). NOAA Tech. Memo. NWS NHC 28, 30 pp.

INITIAL DISTRIBUTION LIST

		No. Copies
1.	Defense Technical Information Center Cameron Station Alexandria, VA 22304-6145	2
2.	Library, Code 0142 Naval Postgraduate School Monterey, CA 93943	2
3.	Chairman (Code 63Rd) Department of Meteorology Naval Postgraduate School Monterey, CA 93943	1
4.	Professor Russell L. Elsberry (Code 63Es) Department of Meteorology Naval Postgraduate School Monterey, CA 93943	5
5.	Dr. Johnny C.L. Chan (Code 63Cd) Department of Meteorology Naval Postgraduate School Monterey, CA 93943	1
6.	Capt Thomas Schott, USAF AWS HQ/DN Scott AFB, IL 62225	3
7.	Director Naval Oceanography Division Naval Observatory 34th and Massachusetts Ave NW Washington, DC 20390	1
8.	Dr. Ted Tsui Naval Environmental Prediction Research Facility Monterey, CA 93943	1
9.	Director Joint Typhoon Warning Center Box 17 FPO San Francisco, CA 96630	1
10.	Commanding Officer Naval Ocean Research and Development Activity NSTL Station Bay St. Louis, MS 39522	1
11.	Commanding Officer Naval Environmental Prediction Research Facility Monterey, CA 93943	1
12.	Chairman, Oceanography Department U.S. Naval Academy Annapolis, MD 21402	1
13.	Chief of Naval Research 800 N. Quincy Street Arlington, VA 22217	1

14. Program Manager (CIRF) 1
Air Force Institute of Technology
Wright-Patterson AFB, OH 45433

15. Air Weather Service 2
Technical Library
Scott AFB, IL 62225

16. Commander 1
Air Weather Service
Scott AFB, IL 62225

17. Commanding Officer 1
Air Force Global Weather Central
Offutt AFB, NE 68113

18. Commanding Officer 1
Naval Oceanography Command Center, Guam
Box 12
FPO San Francisco, CA 96630

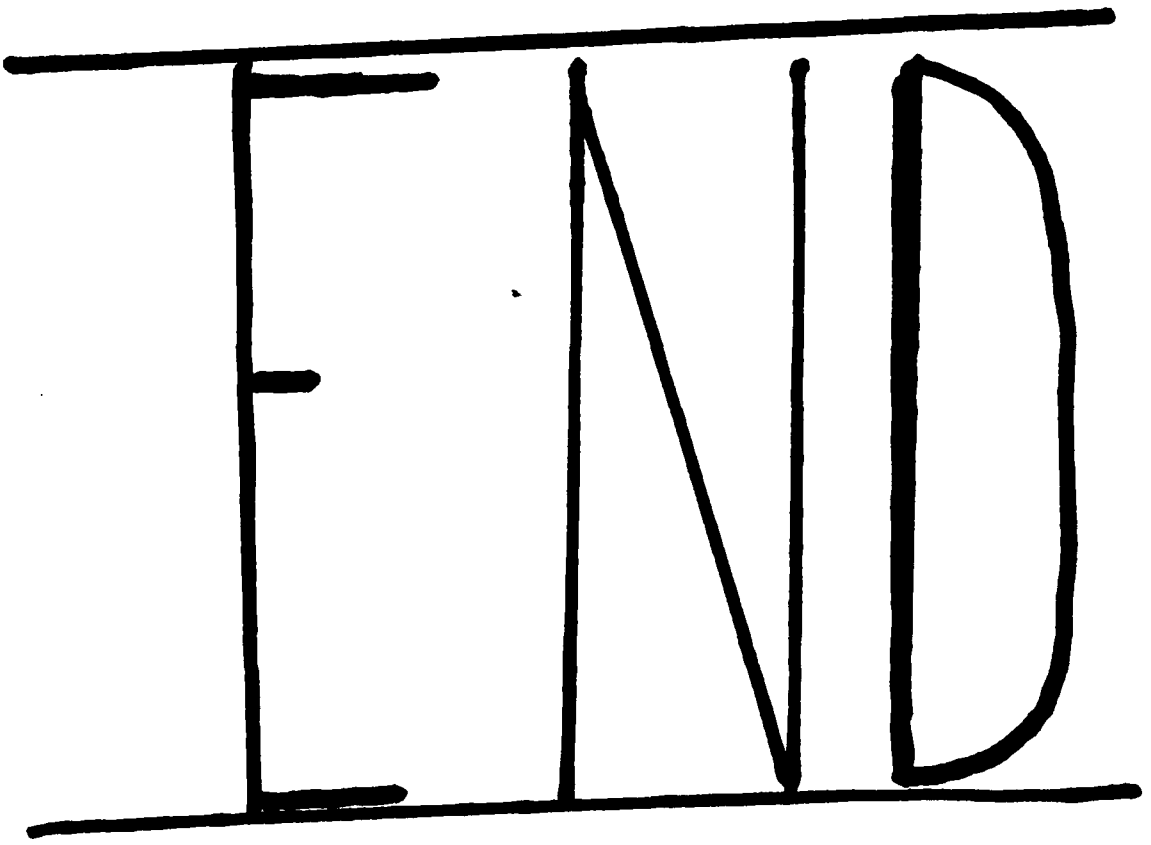

FILMED

3 -86

DTIC